

HAZMAT III: THE UV EVOLUTION OF MID- TO LATE-M STARS WITH *GALEX*

ADAM C. SCHNEIDER¹ AND EVGENYA L. SHKOLNIK¹

¹School of Earth and Space Exploration, Arizona State University, Tempe, AZ, 85282, USA

(Accepted January 19, 2018)

Submitted to AJ

ABSTRACT

Low-mass stars are currently the most promising targets for detecting and characterizing habitable planets in the solar neighborhood. However, the ultraviolet (UV) radiation emitted by such stars can erode and modify planetary atmospheres over time, drastically affecting their habitability. Thus knowledge of the UV evolution of low-mass stars is critical for interpreting the evolutionary history of any orbiting planets. Shkolnik & Barman (2014) used photometry from the *Galaxy Evolution Explorer* (*GALEX*) to show how UV emission evolves for early type M stars ($>0.35 M_{\odot}$). In this paper, we extend their work to include both a larger sample of low-mass stars with known ages as well as M stars with lower masses. We find clear evidence that mid- and late-type M stars (0.08 – $0.35 M_{\odot}$) do not follow the same UV evolutionary trend as early-Ms. Lower mass M stars retain high levels of UV activity up to field ages, with only a factor of 4 decrease on average in *GALEX* NUV and FUV flux density between young (<50 Myr) and old (~ 5 Gyr) stars, compared to a factor of 11 and 31 for early-Ms in NUV and FUV, respectively. We also find that the FUV/NUV flux density ratio, which can affect the photochemistry of important planetary biosignatures, is mass and age-dependent for early Ms, but remains relatively constant for the mid- and late-type Ms in our sample.

Keywords: stars: low-mass

1. INTRODUCTION

As the field of exoplanet exploration has evolved, low-mass stars, or M stars, have taken a prominent position as objects of interest. In addition to being the most abundant stellar constituent in the galaxy ($\sim 75\%$, Bochanski et al. 2010) and commonly having terrestrial planets in their habitable zones (HZs) ($\sim 25\%$; Dressing & Charbonneau 2015), M dwarfs have numerous observational advantages for both the identification and characterization of their planets (see e.g., Shields et al. 2016), which have led to several HZ planet discoveries, including a terrestrial planet around our closest stellar neighbor, the M5.5 dwarf Proxima Cen (Anglada-Escudé et al. 2016), three of seven earth-sized planets around the nearby M8 dwarf TRAPPIST-1 (Gillon et al. 2016, Gillon et al. 2017), and LHS 1140b, a super-earth around an M4.5 dwarf (Dittmann et al. 2017).

However, because M stars have active chromospheres and coronae that produce high-energy radiation that may be harmful for life, with the added complications due to a prolonged pre-main sequence phase (e.g., Tian & Ida 2015) and likely being tidally locked (e.g., Checlair et al. 2017, Barnes 2017), determining the habitability of planets orbiting M stars is not straightforward. The stellar UV flux incident on a planet in an M star's habitable zone may hinder the development extrasolar biology (Ranjan et al. 2017), destroy the very biosignatures we hope to detect, or even lead to the formation of abiotic oxygen and ozone, producing false-positive biosignatures (Domagal-Goldman et al. 2014, Tian et al. 2014, Harman et al. 2015). Thus knowledge of the UV environments of low-mass stars over planet formation and evolution timescales is vital to any investigation of potentially habitable planets in orbit around them.

Ideally, we would be able to obtain high-resolution UV spectra of a large sample of low-mass stars spanning a wide range of masses and ages. However, UV spectroscopy is currently only possible with the *Hubble Space Telescope*, which is highly competitive and would require more orbits than available for such a sample. So far, such observations have been limited to a relatively modest sample (~ 15) of low-mass stars (France et al. 2013, France et al. 2016, Guinan et al. 2016, Youngblood et al. 2017). Alternatively, photometry from the *Galaxy Evolution Explorer* (*GALEX*), which observed approximately two-thirds of the sky with two UV bands centered at mean wavelengths of 1516 Å (FUV) and 2267 Å (NUV)¹, provides an invaluable resource for studying

the UV evolution and properties of a large sample of low-mass stars.

There have been several studies utilizing photometry from *GALEX* to probe stellar evolution, including using enhanced UV flux to identify new nearby, low-mass, young stars (Shkolnik et al. 2011, Rodriguez et al. 2011, Rodriguez et al. 2013, and Kastner et al. 2017), and investigating the age-activity relationship for early type stars (A-K spectral types – Findeisen et al. 2011).

Stelzer et al. (2013) used a volume limited sample of M stars (10 pc) to investigate correlations between *GALEX* and other activity indicators (X-ray and H α emission) and noted a drop in UV flux between young and old M stars. Ansdel et al. (2015) constructed a NUV luminosity function using bright, early-type M dwarfs from Lépine & Gaidos (2011), and confirmed the results of Stelzer et al. (2013) and Shkolnik & Barman (2014) that the base NUV emission for low-mass stars is above that expected from photospheres only. Jones & West (2016) used a sample of M dwarfs from the Palomar/MSU nearby star survey (Reid et al. 1995) and the SDSS DR7 M dwarf spectroscopic sample (West et al. 2011) to construct a correlation between UV luminosities and H α emission and investigate UV emission versus galactic scale height (a proxy for age), and found a decrease in NUV emission with distance from the plane.

The Habitable Zones and M dwarf Activity across Time (HAZMAT) program was initiated specifically to determine the time-dependent habitability around low-mass stars by using UV observations to provide the much needed empirical constraints for the short wavelength regions of low-mass stellar models (Shkolnik & Barman 2014, Miles & Shkolnik 2017). Planet occurrence rates have been shown to increase with decreasing stellar mass (Mulders et al. 2015a), and the planets around low-mass stars are also typically smaller than those around higher-mass stars (Mulders et al. 2015b). Considering that the stellar mass function peaks around M4, or $\sim 0.2 M_{\odot}$ at old ages (Bochanski et al. 2010), mid-Ms may provide the most opportunities and advantageous conditions for detailed characterizations of habitable zone planets through atmospheric spectroscopy. Several known systems with transiting planets orbiting mid- and late-M dwarfs are already planned to be observed with the *James Webb Space Telescope* (e.g., LHS 1140; Dittmann et al. 2017, Trappist-1; Gillon et al. 2016, Gillon et al. 2017), and many more exoplanetary systems around low-mass stars in the Solar neighborhood discovered with the upcoming TESS mission (Ricker et al. 2014, Muirhead et al. 2017, Stassun et al. 2017) will be prime candidates for future atmospheric characterization observations (Batalha et al.

¹ <http://galex.stsci.edu/gr6/?page=faq>

2015, Cowan et al. 2015, Crossfield 2016, Crouzet et al. 2017). In this third installment of the HAZMAT series, we extend the study of the UV environments of low-mass stars at various ages to later spectral types. We describe our sample selection in Section 2, *GALEX* photometry in Section 3, and provide an analysis of the results of this investigation in Section 4.

2. LOW-MASS STAR SAMPLE

We investigated young associations and clusters from Shkolnik & Barman (2014) with confirmed low-mass members. These included the TW Hya Association (10 ± 3 Myr; Bell et al. 2015), the β Pictoris moving group (24 ± 3 Myr; Bell et al. 2015, 26 ± 3 Myr; Nielsen et al. 2016, 22 ± 6 Myr; Shkolnik et al. 2017), the Tucana-Horologium moving group (45 ± 4 Myr; Bell et al. 2015), the AB Doradus Moving Group (149_{-19}^{+51} ; Bell et al. 2015), the Hyades (625 ± 50 Myr; Perryman et al. 1998)², and objects with field ages (~ 5 Gyr).

Members of the TW Hya association were taken from the census of stellar and substellar members in Gagné et al. (2017). The objects included in this study are those labeled in Gagné et al. (2017) as bona fide members and high-likelihood candidate members (>90% probability of belonging to TW Hya). We chose not to use “candidate” TW Hya members from Gagné et al. (2017), because, as stated in that paper, this group may suffer from significant contamination from interlopers. For the β Pictoris Moving Group, we use the member list from Shkolnik et al. (2017) (all “Y” and “Y?” members from Table 4 of that paper). Low-mass confirmed members of the Tucana-Horologium Moving Group come from Kraus et al. (2014). There has not yet been a dedicated census of the low-mass members of the AB Doradus Moving Group, so the members come from multiple sources. References for these sources are provided in Table 5. Hyades members come from Goldman et al. (2013), which expanded the census of Röser et al. (2011) to include more low-mass members using photometry from Pan-STARRS (Kaiser et al. 2002). For field age objects, we use the 8 pc sample of Kirkpatrick et al. (2012) and apply an average age of ~ 5 Gyr, since there are very few pre-main sequence stars known within 8 pc.

The same spectral types corresponds to a different masses at different ages. We determine the corresponding masses for each spectral type for each age by first converting spectral type to effective temperature (T_{eff}).

² Note, however, that Brandt & Huang (2015a) and Brandt & Huang (2015b) determine an age of 750 ± 100 Myr for the Hyades by including rotation in stellar evolution models.

For groups older than 100 Myr, we use Table 5 of Pecaut & Mamajek (2013) to find T_{eff} values for each spectral type from M0 to M9. For the groups younger than 100 Myr, we use Table 6 of Pecaut & Mamajek (2013), which provides adopted T_{eff} values for spectral types of young stars. Note that the spectral type- T_{eff} relations for young stars in Pecaut & Mamajek (2013) only extend to spectral type M5. For spectral types later than M5 for these young groups, we use the spectral type- T_{eff} relation created for late-M members of the TW Hya association in Gagné et al. (2017). We then interpolate the effective temperatures of group members using the low-mass evolutionary models of Baraffe et al. (2015) to estimate masses. Note that the models of Baraffe et al. (2015) have discrete ages; we use the 10 Myr, 25 Myr, 40 Myr, 120 Myr, 625 Myr, and 5 Gyr model grids for TW Hya, β Pic, Tuc-Hor, AB Dor, the Hyades, and the field, respectively. Mass estimates for each spectral type for each age group are given in Table 1.

In this study, we wish to compare the behavior of mid- and late-type M stars to early-Ms, and chose the fully convective boundary as the division between the two samples. This limit is taken to be $0.35 M_{\odot}$ (Chabrier & Baraffe 1997), which according to Table 1, occurs between M2 and M3 for all age groups. We take the hydrogen burning limit ($0.08 M_{\odot}$; Burrows et al. 1997) as the low-mass cutoff for each age group. Taking into consideration typical spectral type uncertainties of ± 0.5 subtypes, this limit corresponds to a spectral type of $\sim M5$ for TW Hya, β Pic, and Tuc-Hor, M6 for AB Dor, and M8 for the Hyades and field age stars. The mass distribution of all stars used in this study is shown in Figure 1.

3. GALEX PHOTOMETRY

All photometry gathered from *GALEX* for this paper was found using the GalexView tool³. We used a $10''$ search radius and proper-motion-corrected coordinates (to epoch 2007) for each object. We exclude all photometry with photometric flags that signal a bright star window reflection, dichroic reflection, detector run proximity, or bright star ghost, as recommended in the *GALEX* documentation⁴. We also exclude all detections with measured magnitudes less than 15 (corresponding to 34 and $108 \text{ counts s}^{-1}$ for FUV and NUV, respectively), which marks the threshold for saturation for both the FUV and NUV detectors (Morrissey et al. 2007). A number of objects were found to be either unresolved in the *GALEX* images, not observed by *GALEX* at all, or

³ <http://galex.stsci.edu/galexview/>

⁴ http://www.galex.caltech.edu/wiki/Public:Documentation/Chapter_103

Table 1. Spectral Type-Mass Estimates (M_{\odot})^a

Spectral Type	TW Hya (10 Myr)	β Pic (24 Myr)	Tuc-Hor (45 Myr)	AB Dor (149 Myr)	Hyades (625 Myr)	Field (~ 5 Gyr)
M0	0.59	0.62	0.60	0.51	0.53	0.53
M1	0.49	0.52	0.52	0.45	0.47	0.47
M2	0.39	0.38	0.38	0.36	0.37	0.37
M3	0.30	0.26	0.26	0.26	0.27	0.26
M4	0.15	0.14	0.14	0.15	0.16	0.16
M5	0.06	0.06	0.07	0.08	0.11	0.11
M6	0.03	0.04	0.05	0.06	0.09	0.09
M7	0.02	0.03	0.04	0.05	0.08	0.09
M8	0.02	0.02	0.03	0.04	0.07	0.08
M9	0.01	0.02	0.02	0.04	0.07	0.08

^aBased on spectral type- T_{eff} relations from Pecaut & Mamajek (2013) and Gagné et al. (2017) and the models of Baraffe et al. (2015).

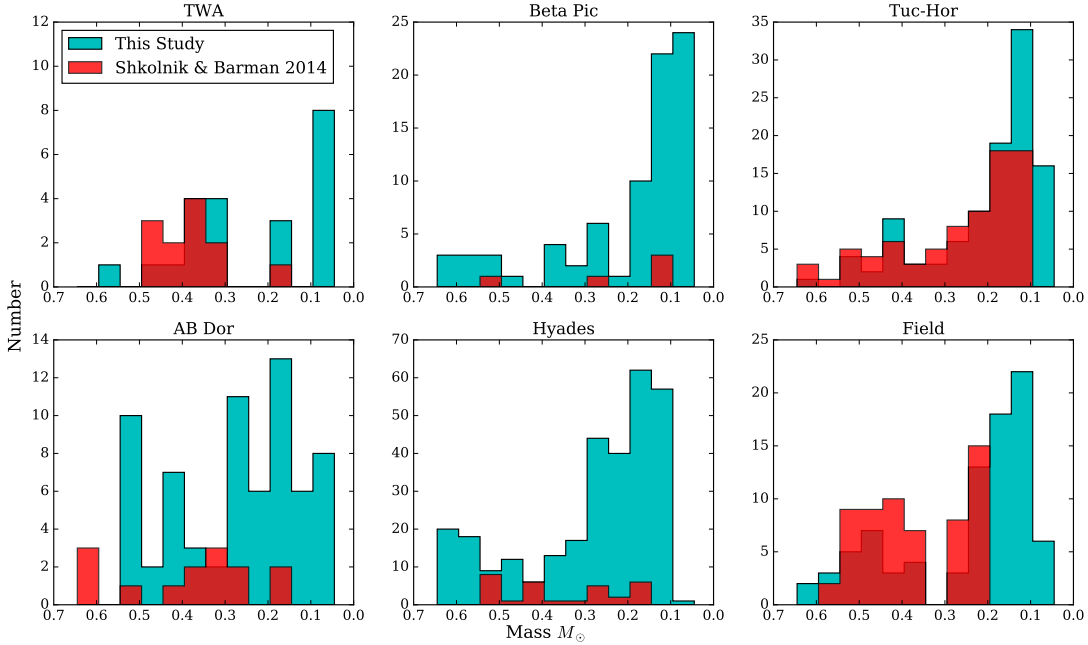


Figure 1. The mass distributions of all stellar groups in this study compared to those of Shkolnik & Barman (2014). The red histograms represent the Shkolnik & Barman (2014) sample, while the cyan histograms represent all objects in this study observed with the *GALEX* NUV passband (i.e., those objects with NUV detections or upper limits).

only had *GALEX* photometry flagged as unreliable in both the FUV and NUV bands. The number of objects in each of these categories for each age group is provided in Table 2. The last column in this table gives the final number of M stars used for each group.

The number of objects observed by *GALEX* and detected in the FUV and NUV *GALEX* bands is given in Table 3. The percentage of objects detected was calculated for the entire sample, early-Ms ($0.35\text{--}0.6 M_{\odot}$), and mid- to late-Ms ($0.08\text{--}0.35 M_{\odot}$). As seen in the table, the fraction of objects detected in the NUV is generally high for each group (>65%). The fraction of stars detected with the FUV band drops significantly for each group compared to NUV detections, most notably for the Hyades. The drop in detections for Hyades members is likely due to a combination of both distance (~ 47 pc; van Leeuwen 2009) and possibly the older age of the cluster. We note that the number of detections in most groups is mass dependent. This is more clearly illustrated in Figure 2, which shows the fraction of stars detected with the NUV and FUV filters as a function of stellar mass for each group.

All *GALEX* NUV and FUV photometry is given in Table 5. In some instances, GalexView will provide multiple detections for a single source, often with varying exposure times. The magnitudes reported in Table 5 are the weighted averages of all detections and the uncertainties are the weighted standard deviations.

If a source was observed by *GALEX* but not detected, we determine an upper limit for that source by first executing a search around that object's position for all objects within a $10'$ radius. We then perform a power-law fit to the relationship between the signal-to-noise ratio (S/N) and the signal of each nearby detection, excluding those objects that exceed the saturation threshold of the detector or with photometric flags listed earlier in this section. We then take the magnitude that a source would have with a S/N of 2 using our power-law fit as an upper limit. These upper limits are provided in Table 5. Note that we do not provide upper limits for sources if they were detected in a different *GALEX* exposure.

Figure 1 compares the sample of objects used in this study that were observed with the *GALEX* NUV passband to those used for these groups in Shkolnik & Barman (2014). Shkolnik & Barman (2014) originally included TWA 31 (M4.2) in their sample of TW Hya members, however this star has since been shown to be a likely nonmember (Schlieder et al. 2012a, Gagné et al. 2017) and is not included in this comparison. As seen in the figure, we have significantly expanded the sample of Shkolnik & Barman (2014), especially at lower masses. The expansion of this sample at early types is largely

due to concerted efforts to identify more low-mass cluster/group members. Note that the HAZMAT I study of Shkolnik & Barman (2014) focused mostly on early Ms, and thus included very few known group members with spectral types later than M4. Since that study, there have been many more investigations targeting and confirming late-M type members of young, nearby moving groups (e.g., Gagné et al. 2015a, Shkolnik et al. 2017).

4. ANALYSIS

4.1. The NUV and FUV Evolution of Low-Mass Stars

To investigate *GALEX* FUV and NUV evolutionary trends, we use flux density values relative to the Two Micron All-Sky Survey (2MASS) *J*-band. We first convert magnitudes to flux densities for *GALEX* data in μJy using:

$$f_{\text{GALEX}} = 10^{\frac{23.9 - (m_{\text{GALEX}})}{2.5}} \quad (1)$$

where m_{GALEX} is either a *GALEX* FUV or NUV magnitude. To convert 2MASS *J* magnitudes to flux densities in μJy :

$$f_{\text{J}} = (1.594 \times 10^9) 10^{\frac{m_{\text{J}}}{-2.5}} \quad (2)$$

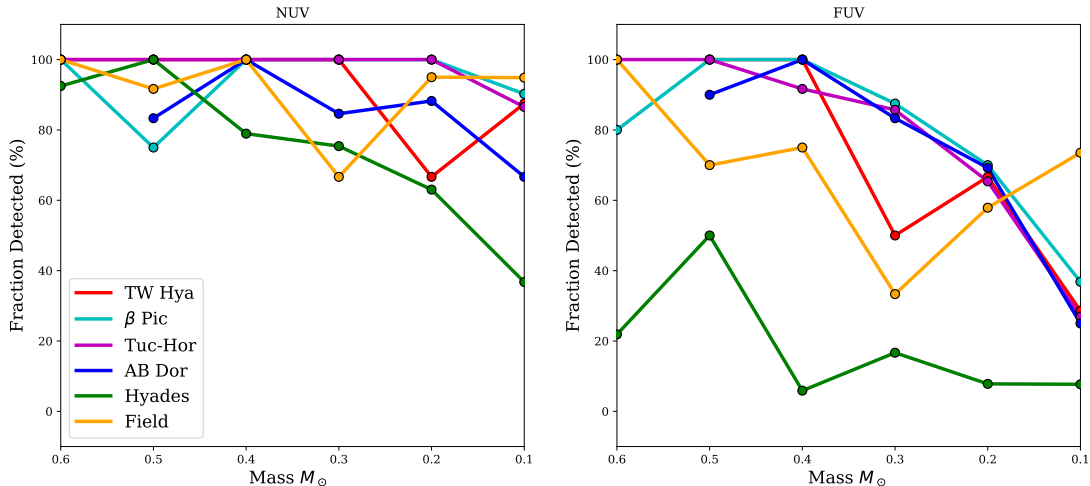
where m_{J} is the 2MASS *J*-band magnitude. In order to understand the evolution of the total UV flux density applicable to exoplanet photochemistry models, we do not subtract the contribution from a model photosphere as in Shkolnik & Barman (2014). The contribution to FUV and NUV flux densities by the stellar photosphere is discussed in more detail in Section 4.4.

If one wishes to convert flux densities to flux values, care should be taken, specifically with the choice of effective wavelengths for the *GALEX* FUV and NUV filters. Determining the effective wavelength of a filter depends on the underlying spectrum of the object being investigated. Effective wavelengths are typically determined using the spectrum of Vega, which differs significantly from an M dwarf spectrum (see Appendix for further discussion).

Figures 3 and 4 show the distribution of NUV and FUV flux density ratios for each age, split into early-type and mid- to late-type M stars. As in Shkolnik & Barman (2014), we see a significant amount of scatter for each group, with ratios typically spanning 1 or 2 orders of magnitude within each age group. The NUV distributions for early-Ms (left panel of Figure 3) display the same trend as seen in Shkolnik & Barman (2014) and Ansdell et al. (2015), very little change in $f_{\text{NUV}}/f_{\text{J}}$ values up until a decrease is seen at Hyades age, and

Table 2. Input Sample Summary

Cluster/Group	Age	Input Sample	Not Observed	Unresolved	Bad Photometry	Final
	(Myr)	Members	By <i>GALEX</i>	in <i>GALEX</i>	Flags in <i>GALEX</i>	Number
		(#)	(#)	(#)	(#)	(#)
TW Hya	10 ± 3	40	4	14	0	22
β Pic	24 ± 3	105	0	25	5	75
Tuc-Hor	45 ± 5	118	13	0	0	105
AB Dor	149_{-19}^{+51}	92	19	7	4	62
Hyades	625 ± 50	450	167	2	8	283
Field	~ 5000	172	41	35	5	91

**Figure 2.** The fraction of objects detected with the *GALEX* NUV (left) and FUV (right) passbands as a function of mass for all of the groups targeted in this study.

an even steeper decline from Hyades to field ages. The distributions of f_{NUV}/f_J values of lower-mass Ms (right panel of Figure 3) have several notable differences. First, the f_{NUV}/f_J ratios for Hyades members are not seen to decrease compared to younger groups. Secondly, the distribution of f_{NUV}/f_J values for field objects span a much larger range than that of field early-Ms. Both of these differences are more clearly seen in Figure 5, which shows f_{NUV}/f_J ratios as a function of age, and Figure 6, which compares the median f_{NUV}/f_J values of early-Ms to mid- and late-Ms.

To account for the upper limits in our dataset, we perform a survival analysis using the Kaplan-Meier estimator (Kaplan & Meier 1958) as implemented in the `lifelines` python package (Davidson-Pilon 2016). We treat the lowest f_{NUV}/f_J values for each group as detections to account for Efron's bias correction (Efron

1967). The 50% values in the resulting empirical cumulative distribution functions are taken as the median values for each group, with 25% and 75% values representing the inner quartiles, which are provided in Table 4. The cumulative distribution functions for early-Ms and mid- to late-Ms for each group are shown in Figure 7.

These values can be used to predict NUV and FUV flux densities for other low-mass stars, or incident flux densities on exoplanetary atmospheres for hypothetical stars. This can be accomplished by determining the J -band flux density of the object of interest, either through photometry or synthetically using a model spectrum and the J -band spectral response curve⁵. Multi-

⁵ https://www.ipac.caltech.edu/2mass/releases/allsky/doc/sec6_4a.html

Table 3. *GALEX* Detection Summary

Cluster/Group	FUV (observed)	FUV (detected)	NUV (observed)	NUV (detected)
Entire Sample				
TW Hya	20	12 (60%)	22	20 (91%)
β Pic	67	38 (57%)	73	69 (95%)
Tuc-Hor	102	55 (54%)	104	96 (92%)
AB Dor	56	41 (73%)	61	53 (87%)
Hyades	203	28 (14%)	280	186 (66%)
Field	78	54 (69%)	86	81 (94%)
Early-Ms ($0.35\text{--}0.6 M_{\odot}$)				
TW Hya	6	6 (100%)	7	7 (100%)
β Pic	12	11 (92%)	13	13 (100%)
Tuc-Hor	19	18 (95%)	19	19 (100%)
AB Dor	21	20 (95%)	21	20 (95%)
Hyades	49	11 (22%)	59	53 (90%)
Field	22	17 (77%)	24	23 (96%)
Mid- to Late-Ms ($0.08\text{--}0.35 M_{\odot}$)				
TW Hya	14	6 (43%)	15	13 (87%)
β Pic	55	27 (49%)	60	56 (93%)
Tuc-Hor	81	37 (46%)	85	77 (91%)
AB Dor	35	21 (60%)	40	30 (75%)
Hyades	154	17 (11%)	221	133 (60%)
Field	56	37 (66%)	62	58 (94%)

plying this J -band flux density by the appropriate flux density ratio in Table 4 will give the NUV flux density at the same distance as the J -band flux density measurement of the star of interest.

The f_{NUV}/f_J values for mid- and late-type field age objects cover a large range of values. We investigated whether or not this spread in f_{NUV}/f_J values was spectral type (or mass) dependent, and found no significant correlation between f_{NUV}/f_J values and mass for field age mid- and late-type Ms. We also investigated whether this spread is related to stellar rotation. We can compare the potential effect of varying rotation rates within our field sample by comparing the rotation period distribution seen for low-mass members of the Hyades (Douglas et al. 2016) to that of field M dwarfs seen in Newton et al. (2017). Douglas et al. (2016) found that

nearly all Hyades stars with masses $\lesssim 0.3 M_{\odot}$ are rapidly rotating, with over 80% of such stars having periods less than 10 days and none having periods longer than 30 days. In contrast, Newton et al. (2017) gathered stellar rotation periods for a sample of nearby M stars from the MEarth Project (Berta et al. 2012), the majority of which should have ages consistent with the field population, and found a much larger spread in rotation periods for stars with masses less than $0.35 M_{\odot}$ (see Figure 3 of that paper). Of the stars in the Newton et al. (2017) sample with masses less than $0.35 M_{\odot}$, $\sim 60\%$ have rotation periods less than 10 days while $\sim 33\%$ have periods greater than 30 days. Thus, at the age of the Hyades, very few mid- to late-Ms have spun down while a significant fraction of mid- to late-Ms have spun down at field ages. However, there are still a substantial amount

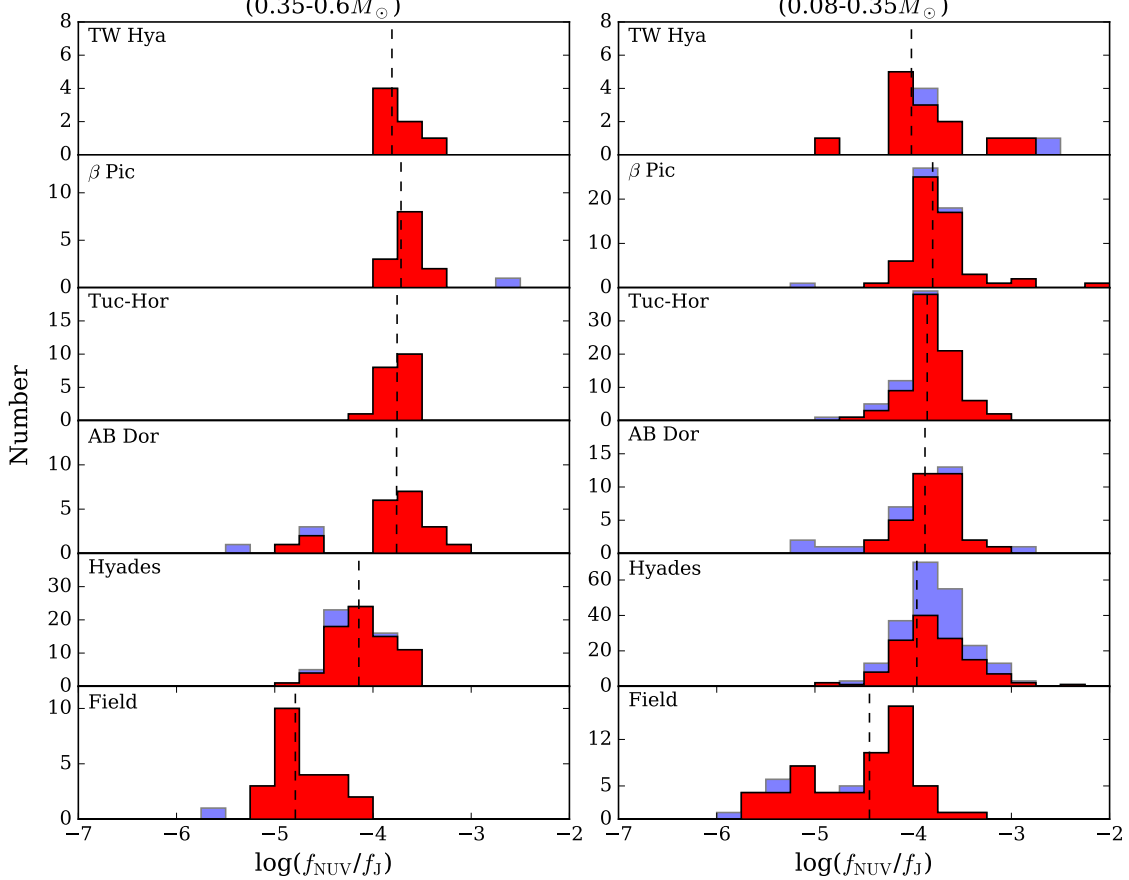


Figure 3. Stacked histograms of the *GALEX* NUV to 2MASS *J* flux density ratios for early (left) and mid- to late- (right) objects in this sample. The red histograms represent detections, while upper limits are shown in blue. Dashed lines represent the median values given in Table 4.

of late-M rapid rotators at field ages, with $\sim 33\%$ having periods less than 1 day. We therefore conclude that the large range of rotation periods measured for mid- to late-Ms in the sample of Newton et al. (2017) is a plausible explanation for the large range of f_{NUV}/f_J values for our field age mid- to late-M sample. This effect is not readily apparent in our early-M sample because the majority early-Ms have spun down at field ages, with $>60\%$ of stars with masses between 0.35 and $0.6 M_\odot$ in the Newton et al. (2017) sample having rotation periods greater than 10 days.

Lastly, the median f_{NUV}/f_J values for field age mid- to late-Ms is significantly higher than that of early-Ms. To compare the survival curves of the early and mid- to late-M samples, we use a log-rank parametric test, which accounts for censored data and tests the null hypothesis that two cumulative distributions have the same parent distribution. The resulting p-values represent the probability that the two populations being compared are drawn from a single distribution. Thus, a low p-value (<0.05) indicates that there is a $>95\%$ probability that

the differences between the population survival curves are not due to random chance. We find that the distributions of f_{NUV}/f_J values for mid- to late-M stars in TW Hya, β Pic, Tuc-Hor, and AB Dor are statistically consistent with the f_{NUV}/f_J values for early-M dwarfs in those groups. For the Hyades and field-age Ms, we find p-values of 0.000 and 0.001, respectively, indicating a significant difference in the distributions of the early-M and mid- to late-M samples. This difference can be seen in Figure 7, where the resulting cumulative distribution functions for these groups are distinct. We find that the median f_{NUV}/f_J ratio decreases by a factor of ~ 4 from Tuc-Hor age (~ 45 Myr) to field ages for mid- to late-Ms, compared to a decrease by a factor of ~ 11 for early-Ms.

For the FUV wavelength region, the evolution of the emission from low-mass stars is similar to that of the NUV, with a few key differences. High-mass Ms in Figure 4 have f_{FUV}/f_J levels that remain relatively consistent until at least the age of AB Dor (149 Myr), with a sharp drop off as field ages are reached, whereas the

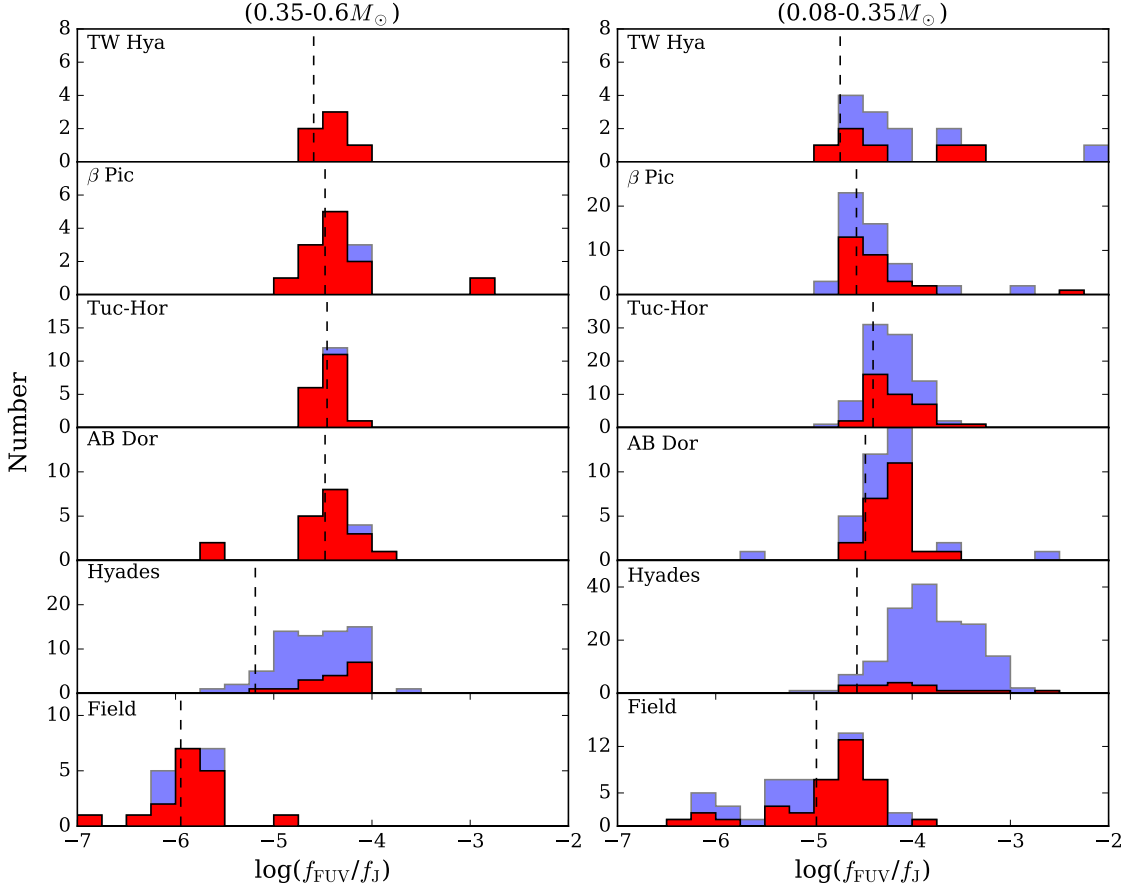


Figure 4. Stacked histograms of the *GALEX* FUV to 2MASS *J* flux density ratio for early (left) and mid- to late- (right) objects in this sample. The red histograms represent detections, while upper limits are shown in blue. Dashed lines represent the median values given in Table 4.

f_{FUV}/f_J values of lower-mass Ms remain relatively constant until Hyades age (625 Myr), with a much smaller drop off toward field ages. Note, however, that the number of detected objects in the FUV in these groups is significantly less than for the NUV, especially for the Hyades (see Table 3).

There is a substantial difference between f_{FUV}/f_J values of early and mid- to late-type field M stars (see Figures 8 and 9). The median f_{FUV}/f_J for early-Ms decreases by a factor of ~ 31 from Tuc-Hor age to field ages, compared to a factor of ~ 4 for mid- to late-Ms. Thus, both NUV and FUV flux density measurements indicate that mid- to late-Ms continue to remain more active with increased UV flux density levels up until field ages compared to early-Ms. A log-rank test comparing the f_{FUV}/f_J distributions of early Ms and mid- to late-Ms again shows that the distributions for young members of TW Hya, β Pic, Tuc-Hor, and AB Dor are not statistically different, while the p-values for the Hyades and field Ms are equal to zero, indicating that these three groups have significantly different samples.

There have been numerous studies of the activity-rotation relationships for low-mass stars showing that more rapidly rotating stars also show higher levels of activity (e.g., Delfosse et al. 1998, Mohanty & Basri 2003, Pizzolato et al. 2003, Kiraga & Stepień 2007, Reiners & Basri 2008, Browning et al. 2010, Kraus et al. 2011, Reiners et al. 2012, West et al. 2015, Houdebine et al. 2016, Stelzer et al. 2016, Astudillo-Defru et al. 2017, Houdebine et al. 2017, Newton et al. 2017). Recent studies of the Hyades (Douglas et al. 2016) and the similarly-aged Praesepe cluster (Douglas et al. 2017) have shown that M stars with spectral types later than $\sim M3$ continue to rotate very rapidly until at least the ages of these clusters. If the mechanism that causes M stars to spin down as they age, typically ascribed to a magnetized stellar wind, does not function efficiently for fully-convective stars, then we would expect them to remain in states of rapid rotation for much longer portions of their lifetimes than early-Ms. Because activity is directly related to rotation, this implies that mid- to late-Ms should remain active for much of their lifetimes.

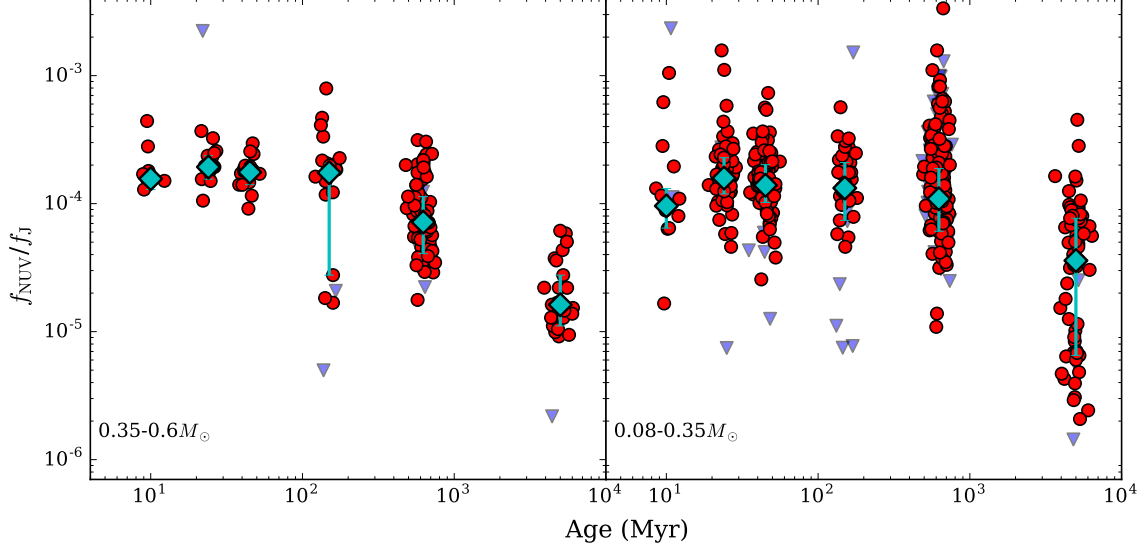


Figure 5. *GALEX* NUV to 2MASS *J* fractional flux density as a function of age for all objects in this sample. Detections are shown as filled red circles, while upper limits are blue triangles. Some symbols are slightly offset along the abscissa for differentiation purposes. The large cyan diamonds represent the median flux density ratios for each age group. Error bars on the medians represent inner quartiles as described in Section 4.1.

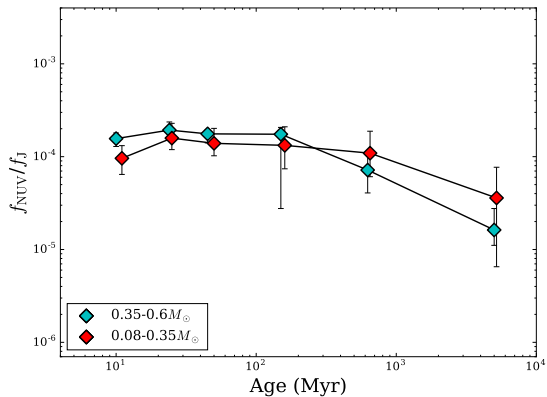


Figure 6. The median *GALEX* NUV to 2MASS *J* fractional flux density as a function of age for early-Ms ($0.35\text{--}0.6 M_{\odot}$; cyan) and mid- to late-Ms ($0.08\text{--}0.35 M_{\odot}$; red). Some symbols are slightly offset along the abscissa for differentiation purposes. Error bars represent inner quartiles as described in Section 4.1.

Thus, the rotation rates of low-mass stars is likely responsible for the *GALEX* UV evolutionary trends that we see.

4.2. Binarity

Another property that can increase activity levels in low-mass stars is binarity (e.g., Morgan et al. 2012). A recent investigation of low-mass stellar activity and rotation using data from K2 showed a clear distinction between activity levels of fast and slow rotators, where those stars with short rotation periods are more active

(Stelzer et al. 2016). They also showed that a substantial number (>40%) of these fast rotators are visual binaries, compared to ~3% for slow rotators. The increased activity levels seen in binaries when compared to single stars is thought to be due to spinning up through tidal interactions or by a reduction in angular momentum loss (Stelzer et al. 2016). Indeed, evidence that binarity affects stellar rotation rates has been seen in several nearby open clusters, including the Pleiades (Covey et al. 2016), the Hyades (Douglas et al. 2016), and Praesepe (Douglas et al. 2017). For this reason, all known visual binaries (VB) and spectroscopic binaries (SB) are flagged in Table 5, with references provided.

In order to investigate whether or not binarity may be biasing any of our results, we split our sample into stars without any evidence of binarity and known spectroscopic binaries or visual binaries with separations smaller than 5'', the FWHM of the *GALEX* NUV band (Morrissey et al. 2007). Figure 10 shows a comparison of the flux density ratios of these samples for every object detected in the NUV. We perform a log-rank test to compare the distributions of binaries versus the rest of each sample and find p-values >0.2 for all groups, consistent with both groups being drawn from the same population. Thus the inclusion of binaries in our evolutionary studies does not bias our results.

4.3. The Relationship Between *GALEX* FUV and NUV For Low-Mass Stars

The FUV to NUV ratio has been suggested to be a major factor affecting the photochemistry of the at-

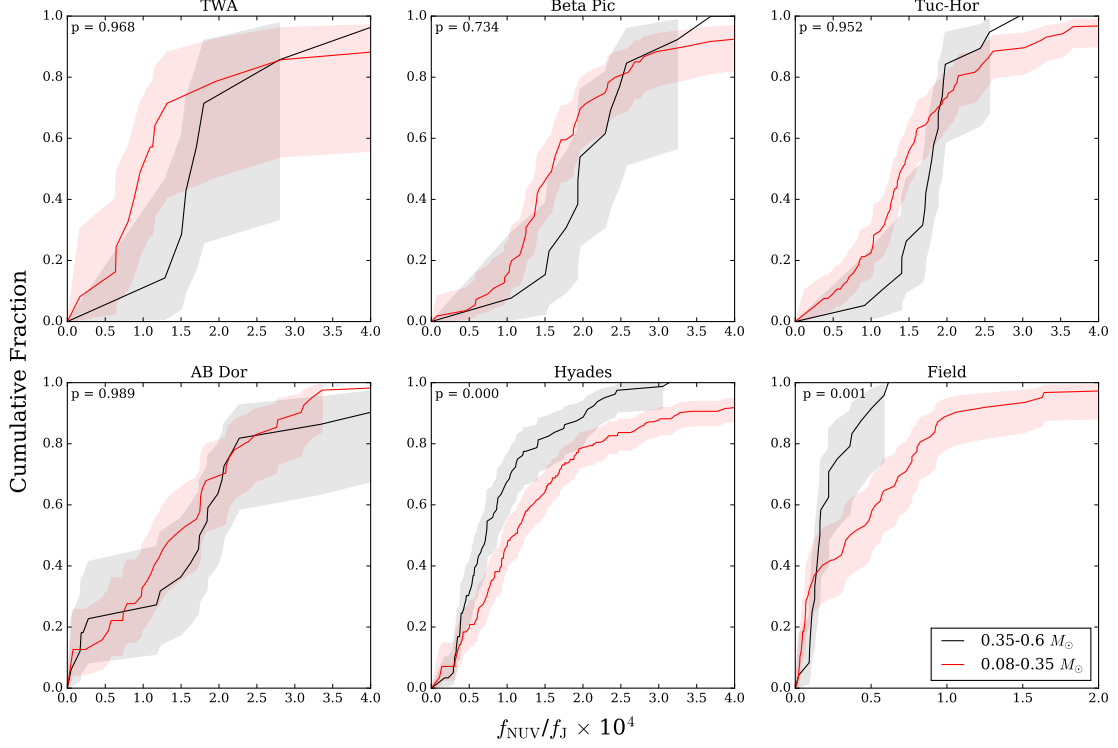


Figure 7. *GALEX* NUV to 2MASS *J* fractional flux density cumulative distribution functions for early-Ms (black) and mid-to late-type Ms (red) for all age groups. The shaded regions represent 1σ confidence intervals for each curve.

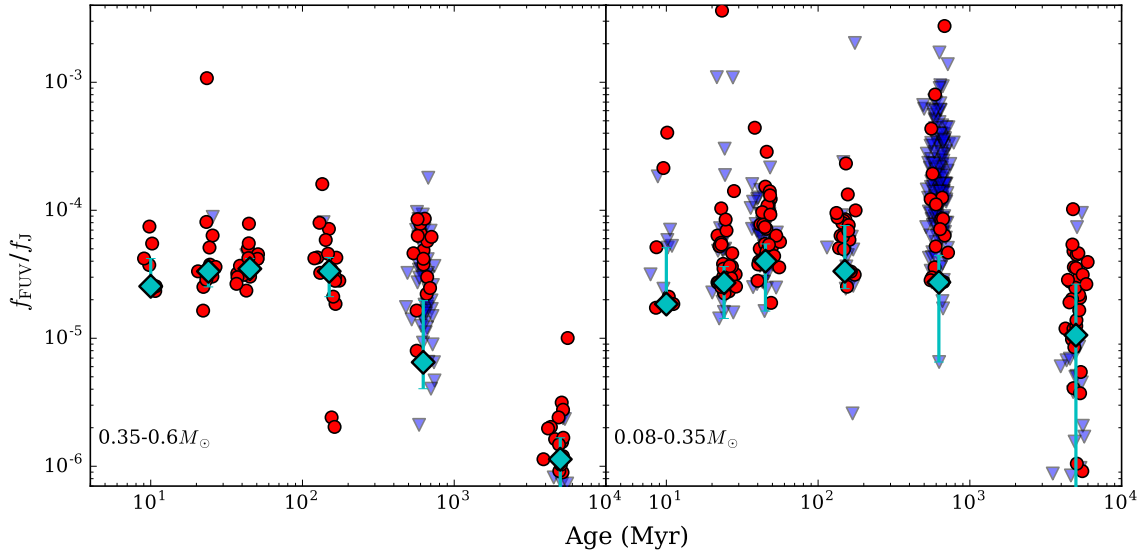


Figure 8. *GALEX* FUV to 2MASS *J* fractional flux density as a function of age for all objects in this sample. Detections are shown as filled red circles, while upper limits are blue triangles. Some symbols are slightly offset along the abscissa for differentiation purposes. The large cyan diamonds represent the median flux density ratios for each age group. Error bars on the medians represent inner quartiles as described in Section 4.1.

Table 4. Median Fractional Flux Densities

Cluster/Group	$f_{\text{FUV}}/f_{\text{J}}^{\text{a}}$	$f_{\text{NUV}}/f_{\text{J}}^{\text{a}}$
Early-Ms ($0.35\text{--}0.6 M_{\odot}$)		
TW Hya (10 Myr)	$2.55\text{e-}05^{+1.65\text{e-}05}_{-2.06\text{e-}06}$	$1.56\text{e-}04^{+2.35\text{e-}05}_{-2.77\text{e-}05}$
β Pic (24 Myr)	$3.33\text{e-}05^{+4.24\text{e-}06}_{-8.15\text{e-}06}$	$1.93\text{e-}04^{+4.32\text{e-}05}_{-3.80\text{e-}05}$
Tuc-Hor (45 Myr)	$3.49\text{e-}05^{+7.02\text{e-}06}_{-4.63\text{e-}06}$	$1.76\text{e-}04^{+1.78\text{e-}05}_{-3.55\text{e-}05}$
AB Dor (149 Myr)	$3.33\text{e-}05^{+9.46\text{e-}06}_{-1.22\text{e-}05}$	$1.74\text{e-}04^{+3.23\text{e-}05}_{-1.47\text{e-}04}$
Hyades (625 Myr)	$6.49\text{e-}06^{+1.33\text{e-}05}_{-2.46\text{e-}06}$ ^b	$7.18\text{e-}05^{+4.18\text{e-}05}_{-3.11\text{e-}05}$
Field (~ 5 Gyr)	$1.13\text{e-}06^{+5.35\text{e-}07}_{-9.57\text{e-}07}$	$1.62\text{e-}05^{+1.14\text{e-}05}_{-5.15\text{e-}06}$
Late-Ms ($0.08\text{--}0.35 M_{\odot}$)		
TW Hya (10 Myr)	$1.85\text{e-}05^{+3.25\text{e-}05}_{-1.20\text{e-}06}$ ^b	$9.60\text{e-}05^{+3.54\text{e-}05}_{-3.16\text{e-}05}$
β Pic (24 Myr)	$2.71\text{e-}05^{+9.20\text{e-}06}_{-1.28\text{e-}05}$	$1.58\text{e-}04^{+7.02\text{e-}05}_{-3.93\text{e-}05}$
Tuc-Hor (45 Myr)	$4.00\text{e-}05^{+1.45\text{e-}05}_{-2.37\text{e-}05}$	$1.39\text{e-}04^{+6.25\text{e-}05}_{-3.70\text{e-}05}$
AB Dor (149 Myr)	$3.34\text{e-}05^{+4.26\text{e-}05}_{-8.99\text{e-}06}$	$1.32\text{e-}04^{+7.74\text{e-}05}_{-5.84\text{e-}05}$
Hyades (625 Myr)	$2.74\text{e-}05^{+1.70\text{e-}05}_{-2.09\text{e-}05}$ ^b	$1.09\text{e-}04^{+7.90\text{e-}05}_{-4.82\text{e-}05}$
Field (~ 5 Gyr)	$1.06\text{e-}05^{+1.59\text{e-}05}_{-1.01\text{e-}05}$	$3.59\text{e-}05^{+4.10\text{e-}05}_{-2.94\text{e-}05}$

^aUncertainties represent inner quartiles of the cumulative distribution functions resulting from the Kaplan-Meier estimator applied to each group.

^bNote that less than 50% of observed objects were detected for these subsamples.

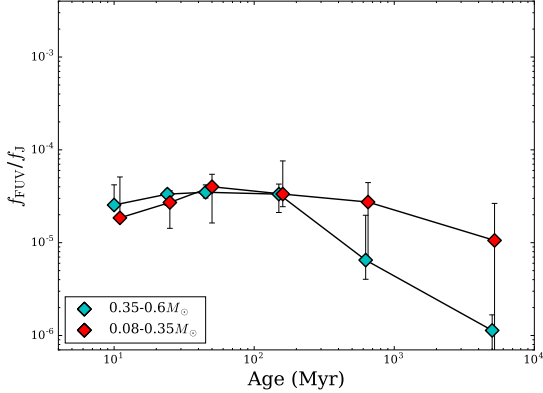


Figure 9. The median *GALEX* FUV to 2MASS *J* fractional flux density as a function of age for $(0.35-0.6 M_\odot$; cyan) and mid- to late-Ms ($0.08-0.35 M_\odot$; red). Some symbols are slightly offset along the abscissa for differentiation purposes. Error bars represent inner quartiles as described in Section 4.1.

mospheres of exoplanets around low-mass stars (e.g., Domagal-Goldman et al. 2014, Tian et al. 2014, Harman et al. 2015). This ratio has been shown to be more than two orders of magnitude from solar-type dwarfs to M dwarfs (France et al. 2013). This change can have a significant influence on the photochemistry of planets around low-mass stars, notably on the abundances of molecules including CO₂, O₂, and O₃. FUV radiation will photolyze CO₂, producing atomic oxygen which can then combine to form O₂ and eventually O₃. NUV radiation on the other hand will dissociate O₃, and thus O₃ abundances are critically dependent on $f_{\text{FUV}}/f_{\text{NUV}}$ values. Therefore, the suggestion of O₃ as a potential biomarker (e.g., Kaltenegger et al. 2007) may not be appropriate for M dwarfs. While the $f_{\text{FUV}}/f_{\text{NUV}}$ ratio has been investigated for several field age stars (France et al. 2013, France et al. 2016), how the $f_{\text{FUV}}/f_{\text{NUV}}$ ratio changes as an M star evolves has not yet been probed.

Our sample of *GALEX*-detected M stars allows us to investigate how the FUV/NUV ratio changes as a function of both mass and age. Note that while the FUV usually refers to the wavelength region extending from 1100–1800Å which includes the most prominent UV emission line (Lyman- α), the *GALEX* FUV band extends from \sim 1350–1800Å, and thus does not include Lyman- α . However, there are still a plethora of strong emission lines that originate in the chromosphere and corona of low-mass stars in the *GALEX* FUV passband, such as Si IV (λ 1394Å), the C IV doublet (λ 1548Å and λ 1551Å), and He II (λ 1640Å), and thus the *GALEX* FUV passband still probes this critical temperature region. We adopt the same nomenclature for the *GALEX* FUV/NUV flux density ratio as Miles & Shkolnik (2017)

($[f_{\text{FUV}}/f_{\text{NUV}}]_G$). Figure 11 shows the $[f_{\text{FUV}}/f_{\text{NUV}}]_G$ values for young stars (TW Hya, β Pic, and Tuc-Hor), AB Dor members, and field stars as a function of mass. We do not include the Hyades because very few Hyades members were detected in the *GALEX* FUV band (see Table 3).

As with f_{NUV}/f_J and f_{FUV}/f_J values, we perform a survival analysis using the Kaplan-Meier estimator to account for the upper limits contained in our dataset. Similar to previous studies (France et al. 2016, Miles & Shkolnik 2017), we find an increase in $[f_{\text{FUV}}/f_{\text{NUV}}]_G$ values as stellar mass decreases for field age M stars. However, we see a clear distinction, by almost an order of magnitude, between young and old early M-type stars. This age difference becomes less apparent as stellar mass decreases, and the two populations are indistinguishable for masses less than $\sim 0.3 M_\odot$. Thus the $[f_{\text{FUV}}/f_{\text{NUV}}]_G$ flux density ratio for mid- and late-type M stars remains relatively constant over their lifetimes, while this ratio clearly evolves to lower values with age for early-type Ms. These larger $[f_{\text{FUV}}/f_{\text{NUV}}]_G$ values for young, early-Ms may have significant consequences on molecular abundances in exoplanet atmospheres at young ages. These different evolutionary patterns should be taken into account when modeling the atmospheres of planets orbiting such stars.

The origin of the different $[f_{\text{FUV}}/f_{\text{NUV}}]_G$ evolutionary patterns between early- and late-Ms can be deduced by comparing the f_{NUV}/f_J and f_{FUV}/f_J ratios discussed in Section 4.1 and seen in Figures 3 through 9. The f_{NUV}/f_J and f_{FUV}/f_J ratios for late-type Ms decrease by a similar amount from young to field ages, resulting in relatively constant $[f_{\text{FUV}}/f_{\text{NUV}}]_G$ ratios across all ages. For early Ms, the f_{FUV}/f_J ratio has a steeper decrease from young to field ages compared to the f_{NUV}/f_J ratio, resulting in an evolving $[f_{\text{FUV}}/f_{\text{NUV}}]_G$ ratio where the contribution to the overall UV from the FUV band becomes less significant as a star ages.

The UV evolutionary difference between young and field-age Ms can also be clearly seen when comparing absolute FUV and NUV flux densities. Using distances for our field sample from Kirkpatrick et al. (2012) and for young Ms (< 50 My; TW Hya, β Pic, and Tuc-Hor) from Kraus et al. (2014), Bell et al. (2015), Gagné et al. (2017), and Shkolnik et al. (2017), we can compare the absolute flux densities for all objects in our sample detected in both the FUV and NUV bands. Figure 12 shows a comparison of absolute flux densities for both young and field-age Ms for objects in our sample detected in both the FUV and NUV bands. While Ms of all masses follow a single trend for young low-mass stars, there is a clear offset between higher and lower-mass Ms

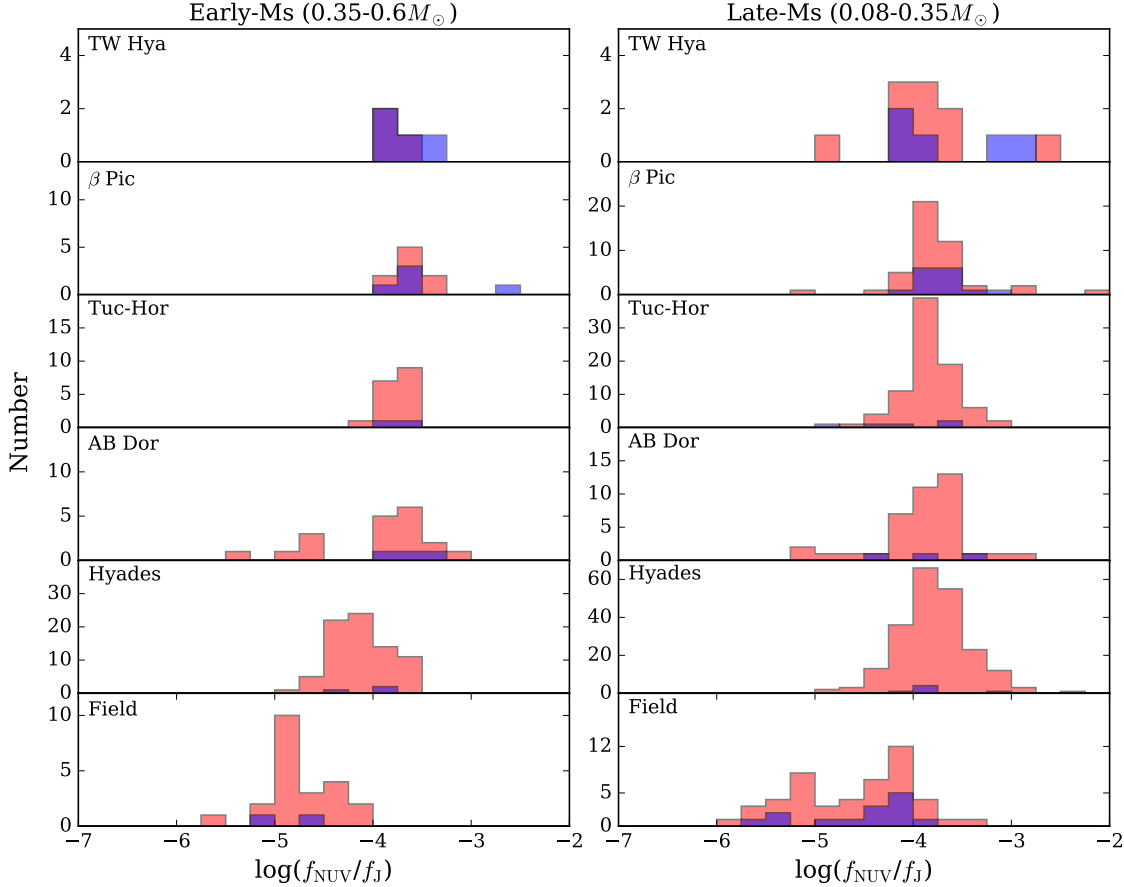


Figure 10. Histograms of the *GALEX* NUV fractional flux densities for stars without evidence of binarity (red) and known binaries (blue), where overlapping areas appear purple.

in the field sample. We perform a least-squares fit to the data using a power law of the following form to find the following relations between f_{FUV} and f_{NUV} for young Ms:

$$f_{\text{FUV}} = 0.56 \pm 0.10(f_{\text{NUV}})^{0.88 \pm 0.03} \quad (3)$$

the following two relations for higher-mass ($> 0.35 M_{\odot}$) and lower-mass ($\leq 0.35 M_{\odot}$) field-age Ms:

$$f_{\text{FUV}} = 0.09 \pm 0.03(f_{\text{NUV}})^{0.96 \pm 0.10}, (M > 0.35 M_{\odot}) \quad (4)$$

$$f_{\text{FUV}} = 0.40 \pm 0.08(f_{\text{NUV}})^{0.93 \pm 0.05}, (M \leq 0.35 M_{\odot}) \quad (5)$$

where f_{FUV} and f_{NUV} are flux densities at 10 pc in μJy . Uncertainties are determined in a Monte Carlo fashion. Note that the power law slopes are all within 1σ combined, while the offsets are significantly different. A hint of this trend was also seen in Miles & Shkolnik (2017). These values can be used for estimating f_{FUV} and f_{NUV} values for objects for which only one or the other is available.

4.4. The Photospheric Contribution to FUV and NUV Flux Densities

One of the primary motivations of this work is to empirically inform low-mass stellar models with measured FUV and NUV flux densities, as stellar models for M-type stars do not include contributions from chromospheres, transition regions, or coronae, though progress is being made to include these components (Peacock et al. 2015, Fontenla et al. 2016). Using existing low-mass stellar evolution models, we can determine how much emission in the *GALEX* FUV and NUV bands is due solely to the photosphere of the star.

We investigate the photospheric contribution as a function of stellar mass and stellar effective temperature using the PHOENIX stellar atmosphere models (Hauschildt et al. 1997, Short & Hauschildt 2005), the field-age 8 pc sample, and young stars from TW Hya, β Pic, and Tuc-Hor with measured distances. Distances for the 8 pc sample come from Kirkpatrick et al. (2012), while distances for young moving group members come

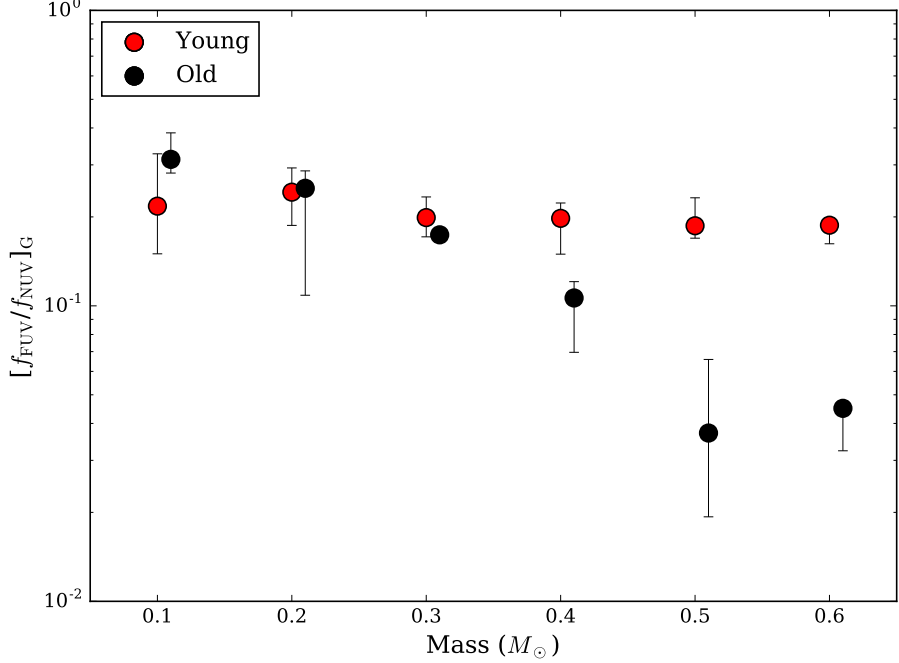


Figure 11. The median *GALEX* FUV/NUV fractional flux density for young M stars (TW Hya, β Pic, and Tuc-Hor) and field-age M stars as a function of mass. Some symbols are slightly offset along the abscissa for differentiation purposes. Error bars represent inner quartiles.

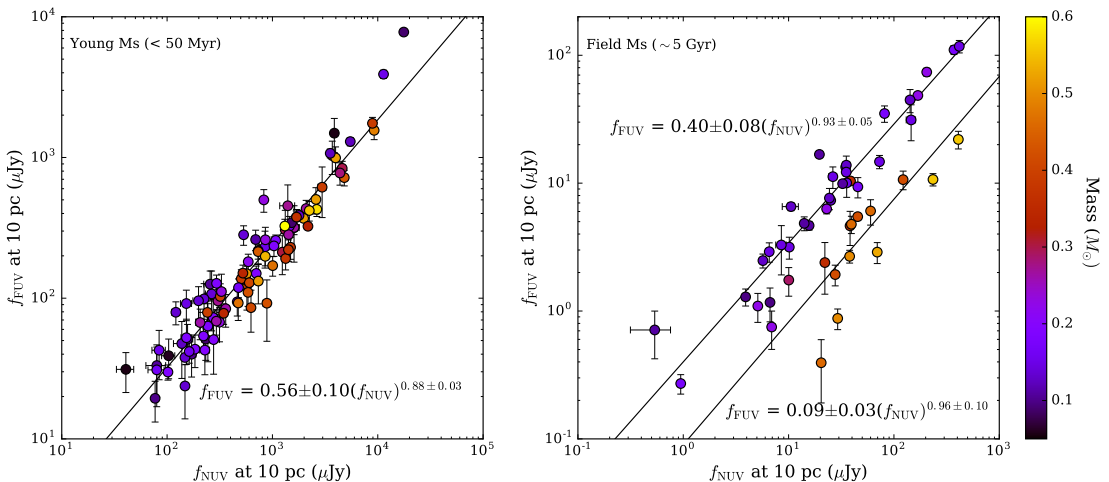


Figure 12. Absolute FUV flux density versus absolute NUV flux density for young (< 50 Myr; left) and field-age (~ 5 Gyr; right) low-mass stars. Black-lines represent least-squares fits to the data. For the field-age sample, we determine separate fits for higher mass ($> 0.35 M_\odot$) and lower-mass ($\leq 0.35 M_\odot$) Ms.

from Kraus et al. (2014), Bell et al. (2015), Gagné et al. (2017), and Shkolnik et al. (2017).

Figure 13 shows the fraction of photospheric flux density to the total observed FUV and NUV flux densities as measured by *GALEX* as a function of both stellar effective temperature and stellar mass. As in Shkolnik & Barman (2014), we find a clear trend with T_{eff} in the FUV for stars between 3400 K and 3800 K, where the

photospheric contribution becomes less significant with decreasing T_{eff} . The inclusion of lower-mass stars from our sample shows that this trend continues for both old and young stars down to at least temperatures of ~ 2800 K, though the distinction between the young and old samples becomes much less clear as T_{eff} decreases. For the NUV, we again find agreement with Shkolnik & Barman (2014) in the 3400 K and 3800 K range, where

the photospheric contribution is relatively constant for both young and old stars. Below ~ 3200 K, a range not probed in Shkolnik & Barman (2014), we find that the photospheric contribution drops considerably for young and old stars, with the two population again becoming indistinct as T_{eff} decreases. Field age Ms in our sample with $T_{\text{eff}} \geq 3200$ K have an average NUV photospheric contribution of $\sim 26\%$, while field age Ms with $T_{\text{eff}} < 3200$ K have an average photospheric contribution of only 0.7%. For the young sample, there is an average $\sim 2\%$ photospheric contribution for $T_{\text{eff}} \geq 3200$ K and 0.7% for $T_{\text{eff}} < 3200$ K. Thus the contribution to the overall flux density in the *GALEX* FUV and NUV bands from the stellar photosphere becomes even less significant for lower-mass M-type stars.

5. CONCLUSIONS

Because UV emission can have severe effects on the compositions, and existence at all, of exoplanet atmospheres orbiting low-mass stars, it is critical to know not only the current state of UV emission from planet hosts, but how emission evolved to its current state. Using *GALEX* photometry and a large sample of nearby, low-mass stars with known ages, we have shown that early-Ms and mid- to late-Ms evolve very differently. Mid- to late-Ms remain relatively active throughout their lifetimes, with only a small UV flux density decrease from young to old ages, whereas early-Ms have a much more significant decrease over the same age range.

GALEX photometry has been shown to correlate with emission from the strongest FUV emission line, Lyman- α (Shkolnik et al. 2014), which dominates the UV spectrum of low-mass stars (e.g., Loyd et al. 2016) and controls the photodissociation of molecules such as O₂, H₂O, CH₄ (e.g., Linsky et al. 2013). Furthermore, FUV flux has been shown to be strongly correlated to X-ray and EUV flux (Shkolnik & Barman 2014, Mitra-Kraev et al. 2005, France et al. 2016), which controls much of the upper atmospheric heating of orbiting planets (e.g.,

Lammer et al. 2007, Tian 2009). Thus, the prolonged UV activity seen for low-mass Ms, which we attribute to different rotation rates for early-Ms and fully convective mid- to late-Ms, can have serious consequences for the potential habitability and the detection of such habitability of Proxima Cen b (Anglada-Escudé et al. 2016) and LHS 1140b (Dittmann et al. 2017), and the planets around TRAPPIST-1 (Gillon et al. 2016, Gillon et al. 2017), which orbit M5.5, M4.5, and M8 stars, respectively.

A. S. and E. S. appreciate support from NASA/Habitable Worlds grant NNX16AB62G (PI E. Shkolnik). The results reported herein benefited from collaborations and/or information exchange within NASA’s Nexus for Exoplanet System Science (NExSS) research coordination network sponsored by NASA’s Science Mission Directorate and the NExSS grant NNX15AD53G (PI S. Desch). We wish to thank the anonymous referee for a helpful report that improved the quality of this work. We thank Victoria Meadows, Travis Barman, David Charbonneau, Zach Berta-Thompson, Taisiya Kopytova, Kim Ward-Duong, and Jennifer Patience for useful discussions. This work is based on observations made with the NASA Galaxy Evolution Explorer. *GALEX* is operated for NASA by the California Institute of Technology under NASA contract NAS5-98034. This publication makes use of data products from the Two Micron All Sky Survey, which is a joint project of the University of Massachusetts and the Infrared Processing and Analysis Center/California Institute of Technology, funded by the National Aeronautics and Space Administration and the National Science Foundation. This research has made use of the SIMBAD database, operated at CDS, Strasbourg, France. This research has made use of the Washington Double Star Catalog maintained at the U.S. Naval Observatory.

REFERENCES

- Alonso-Floriano, F. J., Caballero, J. A., Cortés-Contreras, M., Solano, E., & Montes, D. 2015, A&A, 583, A85
- Anglada-Escudé, G., Amado, P. J., Barnes, J., et al. 2016, Nature, 536, 437
- Ansdell, M., Gaidos, E., Mann, A. W., et al. 2015, ApJ, 798, 41
- Artigau, É., Gagné, J., Faherty, J., et al. 2015, ApJ, 806, 254
- Astudillo-Defru, N., Delfosse, X., Bonfils, X., et al. 2017, A&A, 600, A13
- Baraffe, I., Homeier, D., Allard, F., & Chabrier, G. 2015, A&A, 577, A42
- Barnes, R. 2017, Celestial Mechanics and Dynamical Astronomy,
- Barrado y Navascués, D., Stauffer, J. R., & Patten, B. M. 1999, ApJL, 522, L53
- Batalha, N., Kalirai, J., Lunine, J., Clampin, M., & Lindler, D. 2015, arXiv:1507.02655
- Bell, C. P. M., Mamajek, E. E., & Naylor, T. 2015, MNRAS, 454, 593

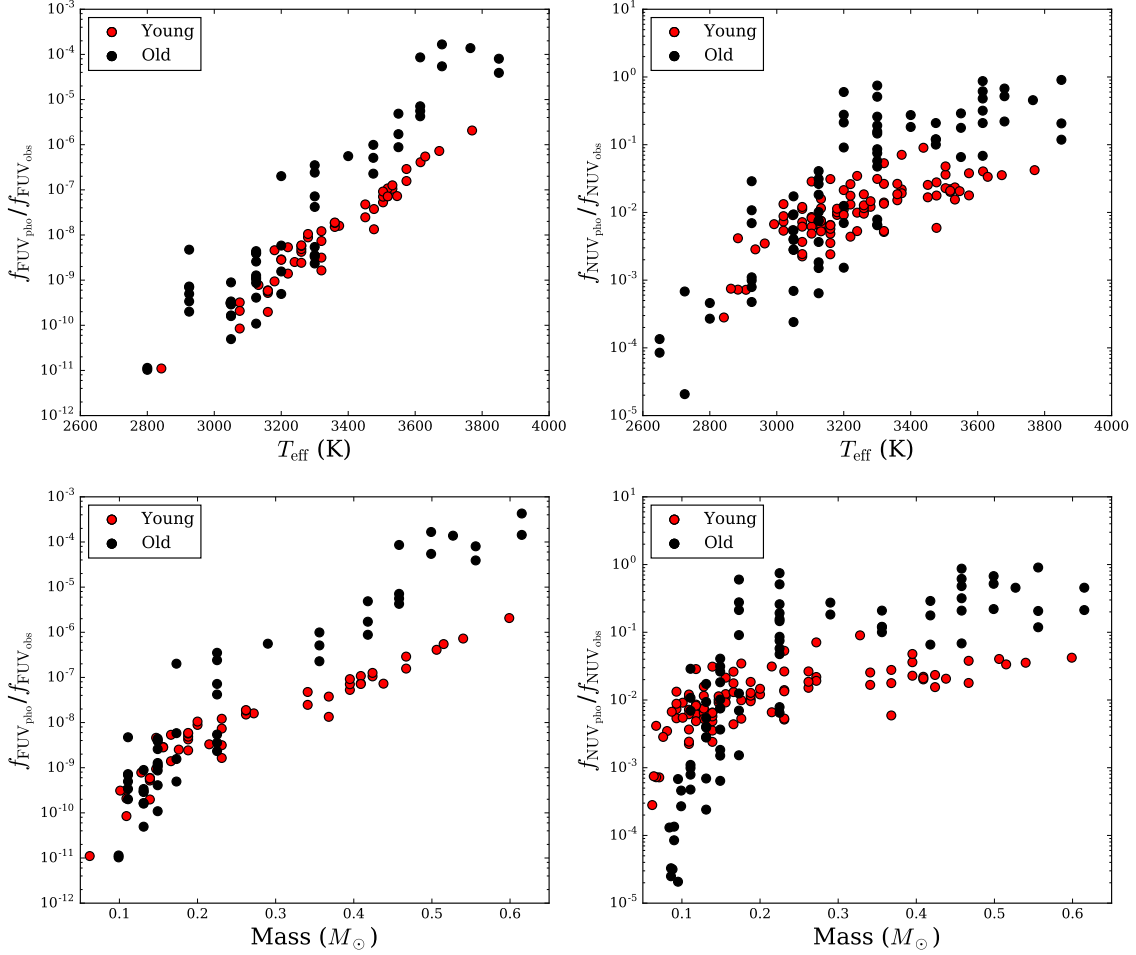


Figure 13. The fraction of observed FUV (left) and NUV (right) flux density from the stellar photosphere as a function of stellar effective temperature (top) and stellar mass (bottom).

- Bender, C. F., & Simon, M. 2008, ApJ, 689, 416-429
 Bergfors, C., Brandner, W., Janson, M., et al. 2010, A&A, 520, A54
 Berta, Z. K., Irwin, J., Charbonneau, D., Burke, C. J., & Falco, E. E. 2012, AJ, 144, 145
 Binks, A. S., Jeffries, R. D., & Maxted, P. F. L. 2015, MNRAS, 452, 173
 Binks, A. S., & Jeffries, R. D. 2016, MNRAS, 455, 3345
 Bochanski, J. J., Hawley, S. L., Covey, K. R., et al. 2010, AJ, 139, 2679-2699
 Bouvier, J., Kendall, T., Meeus, G., et al. 2008, A&A, 481, 661
 Bowler, B. P., Liu, M. C., Shkolnik, E. L., et al. 2012, ApJ, 753, 142
 Bowler, B. P., Liu, M. C., Shkolnik, E. L., & Dupuy, T. J. 2013, ApJ, 774, 55
 Bowler, B. P., Liu, M. C., Shkolnik, E. L., & Tamura, M. 2015, ApJS, 216, 7
 Brandt, T. D., & Huang, C. X. 2015, ApJ, 807, 24

- Brandt, T. D., & Huang, C. X. 2015, ApJ, 807, 58
 Browning, M. K., Basri, G., Marcy, G. W., West, A. A., & Zhang, J. 2010, AJ, 139, 504
 Burrows, A., Marley, M., Hubbard, W. B., et al. 1997, ApJ, 491, 856
 Chabrier, G., & Baraffe, I. 1997, A&A, 327, 1039
 Chauvin, G., Lagrange, A.-M., Bonavita, M., et al. 2010, A&A, 509, A52
 Checlair, J., Menou, K., & Abbot, D. S. 2017, ApJ, 845, 132
 Covey, K. R., Agüeros, M. A., Law, N. M., et al. 2016, ApJ, 822, 81
 Cowan, N. B., Greene, T., Angerhausen, D., et al. 2015, PASP, 127, 311
 Crain, J. N., Sanders, W. L., Fomalont, E. B., & Sramek, R. A. 1986, PASP, 98, 325
 Crossfield, I. J. M. 2016, arXiv:1604.06458
 Crouzet, N., Bonfils, X., Delfosse, X., et al. 2017, arXiv:1701.03539

- Davidson-Pilon, C. 2016, Lifelines, <https://github.com/camdaavdisonpilon/lifelines>
- Delfosse, X., Forveille, T., Perrier, C., & Mayor, M. 1998, A&A, 331, 581
- Delfosse, X., Forveille, T., Beuzit, J.-L., et al. 1999, A&A, 344, 897
- Delorme, P., Gagné, J., Girard, J. H., et al. 2013, A&A, 553, L5
- Dittmann, J. A., Irwin, J. M., Charbonneau, D., et al. 2017, Nature, 544, 333
- Domagal-Goldman, S. D., Segura, A., Claire, M. W., Robinson, T. D., & Meadows, V. S. 2014, ApJ, 792, 90
- Donaldson, J. K., Weinberger, A. J., Gagné, J., et al. 2016, ApJ, 833, 95
- Douglas, S. T., Agüeros, M. A., Covey, K. R., et al. 2016, ApJ, 822, 47
- Douglas, S. T., Agüeros, M. A., Covey, K. R., & Kraus, A. 2017, ApJ, 842, 83
- Dressing, C. D., & Charbonneau, D. 2015, ApJ, 807, 45
- Efron, R. 1967, Proc. fifth Berkeley Symp. Mathematical Statistics and Probability (Berkeley, CA: Univ. California Press) 4, 831
- Eggen, O. J. 1956, AJ, 61, 405
- Eggen, O. J. 1993, AJ, 106, 1885
- Elliott, P., Bayo, A., Melo, C. H. F., et al. 2014, A&A, 568, A26
- Elliott, P., Bayo, A., Melo, C. H. F., et al. 2016, A&A, 590, A13
- Findeisen, K., Hillenbrand, L., & Soderblom, D. 2011, AJ, 142, 23
- Fischer, D. A., & Marcy, G. W. 1992, ApJ, 396, 178
- Fontenla, J. M., Linsky, J. L., Witbrod, J., et al. 2016, ApJ, 830, 154
- France, K., Froning, C. S., Linsky, J. L., et al. 2013, ApJ, 763, 149
- France, K., Parke Loyd, R. O., Youngblood, A., et al. 2016, ApJ, 820, 89
- Gagné, J., Lafrenière, D., Doyon, R., Malo, L., & Artigau, É. 2014, ApJ, 783, 121
- Gagné, J., Faherty, J. K., Cruz, K. L., et al. 2015a, ApJS, 219, 33
- Gagné, J., Lafrenière, D., Doyon, R., Malo, L., & Artigau, É. 2015b, ApJ, 798, 73
- Gagné, J., Faherty, J. K., Mamajek, E. E., et al. 2017, ApJS, 228, 18
- Gálvez, M. C., Montes, D., Fernández-Figueroa, M. J., & López-Santiago, J. 2006, Ap&SS, 304, 59
- Giclas, H. L., Burnham, R., & Thomas, N. G. 1962, Lowell Observatory Bulletin, 5, 257
- Giclas, H. L., Burnham, R., & Thomas, N. G. 1965, Lowell Observatory Bulletin, 6, 155
- Gillon, M., Jehin, E., Lederer, S. M., et al. 2016, Nature, 533, 221
- Gillon, M., Triaud, A. H. M. J., Demory, B.-O., et al. 2017, Nature, 542, 456
- Gliese, W., & Jahreiß, H. 1979, A&AS, 38,
- Gliese, W., & Jahreiß, H. 1991, On: The Astronomical Data Center CD-ROM: Selected Astronomical Catalogs, Vol. I; L.E. Brotzmann, S.E. Gesser (eds.), NASA/Astronomical Data Center, Goddard Space Flight Center, Greenbelt, MD, I,
- Goldman, B., Röser, S., Schilbach, E., et al. 2013, A&A, 559, A43
- Golimowski, D. A., Henry, T. J., Krist, J. E., et al. 2004, AJ, 128, 1733
- Guenther, E. W., Paulson, D. B., Cochran, W. D., et al. 2005, A&A, 442, 1031
- Guinan, E. F., Engle, S. G., & Durbin, A. 2016, ApJ, 821, 81
- Güntzel-Lingner, U. 1955, Astronomische Nachrichten, 282, 183
- Hanson, R. B. 1975, AJ, 80, 379
- Harman, C. E., Schwierman, E. W., Schottelkotte, J. C., & Kasting, J. F. 2015, ApJ, 812, 137
- Harrington, R. S. 1971, AJ, 76, 930
- Hartkopf, W. I., Mason, B. D., Finch, C. T., et al. 2013, AJ, 146, 76
- Hauschildt, P. H., Baron, E., & Allard, F. 1997, ApJ, 483, 390
- Heintz, W. D. 1987, ApJS, 65, 161
- Helminiak, K. G., Konacki, M., RóŻyczka, M., et al. 2012, MNRAS, 425, 1245
- Henry, T. J., Franz, O. G., Wasserman, L. H., et al. 1999, ApJ, 512, 864
- Herschel, J. F. W., Sir 1847, London, Smith, Elder and co., 1847.,
- Hopmann, J. 1948, ZA, 24, 263
- Houdebine, E. R., Mullan, D. J., Paletou, F., & Gebran, M. 2016, ApJ, 822, 97
- Houdebine, E. R., Mullan, D. J., Bercu, B., Paletou, F., & Gebran, M. 2017, ApJ, 837, 96
- Ianna, P. A. 1979, AJ, 84, 127
- Innes, R. T. A. 1915, Circular of the Union Observatory Johannesburg, 30, 235
- Janson, M., Hormuth, F., Bergfors, C., et al. 2012, ApJ, 754, 44
- Janson, M., Durkan, S., Hippler, S., et al. 2017, A&A, 599, A70

- Jao, W.-C., Henry, T. J., Subasavage, J. P., et al. 2003, AJ, 125, 332
- Jayawardhana, R., Coffey, J., Scholz, A., Brandeker, A., & van Kerkwijk, M. H. 2006, ApJ, 648, 1206
- Jeffers, H. M., van den Bos, W. H., & Greeby, F. M. 1963, Publications of the Lick Observatory, Mount Hamilton: University of California, Lick Observatory, —c1963,
- Johnson, H. L., Mitchell, R. I., & Iriarte, B. 1962, ApJ, 136, 75
- Jones, D. O., & West, A. A. 2016, ApJ, 817, 1
- Kaiser, N., Aussel, H., Burke, B. E., et al. 2002, Proc. SPIE, 4836, 154
- Kaltenegger, L., Traub, W. A., & Jucks, K. W. 2007, ApJ, 658, 598
- Kaplan, E. L., & Meier, P. 1958, J. Am. Stat. Assoc., 53, 457
- Kastner, J. H., Zuckerman, B., Weintraub, D. A., & Forveille, T. 1997, Science, 277, 67
- Kastner, J. H., Sacco, G., Rodriguez, D., et al. 2017, ApJ, 841, 73
- Kiraga, M., & Stepień, K. 2007, AcA, 57, 149
- Kirkpatrick, J. D., Gelino, C. R., Cushing, M. C., et al. 2012, ApJ, 753, 156
- Kiss, L. L., Moór, A., Szalai, T., et al. 2011, MNRAS, 411, 117
- Konopacky, Q. M., Ghez, A. M., Duchêne, G., McCabe, C., & Macintosh, B. A. 2007, AJ, 133, 2008
- Kopytova, T. G., Brandner, W., Tognelli, E., et al. 2016, A&A, 585, A7
- Kraus, A. L., Tucker, R. A., Thompson, M. I., Craine, E. R., & Hillenbrand, L. A. 2011, ApJ, 728, 48
- Kraus, A. L., Shkolnik, E. L., Allers, K. N., & Liu, M. C. 2014, AJ, 147, 146
- Lammer, H., Lichtenegger, H. I. M., Kulikov, Y. N., et al. 2007, Astrobiology, 7, 185
- Law, N. M., Hodgkin, S. T., & Mackay, C. D. 2006, MNRAS, 368, 1917
- Law, N. M., Hodgkin, S. T., & Mackay, C. D. 2008, MNRAS, 384, 150
- Leinert, C., Haas, M., & Jahreiss, H. 1986, A&A, 164, L29
- Leinert, C., Weitzel, N., Richichi, A., Eckart, A., & Tacconi-Garman, L. E. 1994, A&A, 291, L47
- Lépine, S., & Simon, M. 2009, AJ, 137, 3632
- Lépine, S., & Gaidos, E. 2011, AJ, 142, 138
- Linsky, J. L., France, K., & Ayres, T. 2013, ApJ, 766, 69
- Looper, D. L., Mohanty, S., Bochanski, J. J., et al. 2010a, ApJ, 714, 45
- Looper, D. L., Bochanski, J. J., Burgasser, A. J., et al. 2010b, AJ, 140, 1486
- Lowrance, P. J., Becklin, E. E., Schneider, G., et al. 2005, AJ, 130, 1845
- Loyd, R. O. P., France, K., Youngblood, A., et al. 2016, ApJ, 824, 102
- Luyten, W. J. 1997, VizieR Online Data Catalog, 1130,
- Malo, L., Doyon, R., Lafrenière, D., et al. 2013, ApJ, 762, 88
- Malo, L., Artigau, É., Doyon, R., et al. 2014, ApJ, 788, 81
- Mason, B. D., Wycoff, G. L., Hartkopf, W. I., Douglass, G. G., & Worley, C. E. 2001, AJ, 122, 3466
- McCarthy, C., Zuckerman, B., & Becklin, E. E. 2001, AJ, 121, 3259
- McCarthy, K., & White, R. J. 2012, AJ, 143, 134
- Messina, S., Desidera, S., Turatto, M., Lanzafame, A. C., & Guinan, E. F. 2010, A&A, 520, A15
- Messina, S., Millward, M., Buccino, A., et al. 2017a, A&A, 600, A83
- Messina, S., Lanzafame, A. C., Malo, L., et al. 2017, A&A, 607, A3
- Miles, B. E., & Shkolnik, E. L. 2017, AJ, 154, 67
- Miret, X., & Tobal, T. 2009, Double Star Section Circulars, 17, 67
- Mitra-Kraev, U., Harra, L. K., Güdel, M., et al. 2005, A&A, 431, 679
- Mohanty, S., & Basri, G. 2003, ApJ, 583, 451
- Montagnier, G., Ségransan, D., Beuzit, J.-L., et al. 2006, A&A, 460, L19
- Morgan, D. P., West, A. A., Garcés, A., et al. 2012, AJ, 144, 93
- Morrissey, P., Conrow, T., Barlow, T. A., et al. 2007, ApJS, 173, 682
- Muirhead, P. S., Dressing, C., Mann, A. W., et al. 2017, arXiv:1710.00193
- Mulders, G. D., Pascucci, I., & Apai, D. 2015a, ApJ, 798, 112
- Mulders, G. D., Pascucci, I., & Apai, D. 2015b, ApJ, 814, 130
- Nakajima, T., Morino, J.-I., & Fukagawa, M. 2010, AJ, 140, 713
- Newton, E. R., Irwin, J., Charbonneau, D., et al. 2017, ApJ, 834, 85
- Nicholson, M. P. 2015, VizieR Online Data Catalog, 1330,
- Nielsen, E. L., De Rosa, R. J., Wang, J., et al. 2016, AJ, 152, 175
- Pasquini, L., Schmitt, J. H. M. M., Harnden, F. R., Jr., Tozzi, G. P., & Krautter, J. 1989, A&A, 218, 187
- Peacock, S., Barman, T., & Shkolnik, E. 2015, AAS/Division for Planetary Sciences Meeting Abstracts, 47, 404.06
- Pecaut, M. J., & Mamajek, E. E. 2013, ApJS, 208, 9

- Pels, G., Oort, J. H., & Pels-Kluyver, H. A. 1975, *A&A*, 43, 423
- Perryman, M. A. C., Brown, A. G. A., Lebreton, Y., et al. 1998, *A&A*, 331, 81
- Pizzolato, N., Maggio, A., Micela, G., Sciortino, S., & Ventura, P. 2003, *A&A*, 397, 147
- Ranjan, S., Wordsworth, R., & Sasselov, D. D. 2017, *ApJ*, 843, 110
- Reid, N. 1992, *MNRAS*, 257, 257
- Reid, N. 1993, *MNRAS*, 265, 785
- Reid, I. N., Hawley, S. L., & Gizis, J. E. 1995, *AJ*, 110, 1838
- Reid, I. N., & Gizis, J. E. 1997, *AJ*, 114, 1992
- Reid, N. 2003, *MNRAS*, 342, 837
- Reid, I. N., & Mahoney, S. 2000, *MNRAS*, 316, 827
- Reid, I. N., & Walkowicz, L. M. 2006, *PASP*, 118, 671
- Reiners, A., & Basri, G. 2008, *ApJ*, 684, 1390-1403
- Reiners, A., Joshi, N., & Goldman, B. 2012, *AJ*, 143, 93
- Reipurth, B., & Mikkola, S. 2015, *AJ*, 149, 145
- Reuyl, D. 1941, *PASP*, 53, 336
- Ricker, G. R., Winn, J. N., Vanderspek, R., et al. 2014, *Proc. SPIE*, 9143, 914320
- Riedel, A. R. 2012, Ph.D. Thesis,
- Riedel, A. R., Finch, C. T., Henry, T. J., et al. 2014, *AJ*, 147, 85
- Riedel, A. R., Alam, M. K., Rice, E. L., Cruz, K. L., & Henry, T. J. 2017, *ApJ*, 840, 87
- Rodriguez, D. R., Bessell, M. S., Zuckerman, B., & Kastner, J. H. 2011, *ApJ*, 727, 62
- Rodriguez, D. R., Zuckerman, B., Kastner, J. H., et al. 2013, *ApJ*, 774, 101
- Rodriguez, D. R., Zuckerman, B., Faherty, J. K., & Vican, L. 2014, *A&A*, 567, A20
- Röser, S., Schilbach, E., Piskunov, A. E., Kharchenko, N. V., & Scholz, R.-D. 2011, *A&A*, 531, A92
- Schneider, A., Melis, C., & Song, I. 2012a, *ApJ*, 754, 39
- Schneider, A., Song, I., Melis, C., Zuckerman, B., & Bessell, M. 2012b, *ApJ*, 757, 163
- Schlieder, J. E., Lépine, S., & Simon, M. 2010, *AJ*, 140, 119
- Schlieder, J. E., Lépine, S., & Simon, M. 2012a, *AJ*, 143, 80
- Schlieder, J. E., Lépine, S., & Simon, M. 2012b, *AJ*, 144, 109
- Shan, Y., Yee, J. C., Bowler, B. P., et al. 2017, *ApJ*, 846, 93
- Shields, A. L., Ballard, S., & Johnson, J. A. 2016, *PhR*, 663, 1
- Shkolnik, E. L., Liu, M. C., Reid, I. N., Dupuy, T., & Weinberger, A. J. 2011, *ApJ*, 727, 6
- Shkolnik, E. L., Anglada-Escudé, G., Liu, M. C., et al. 2012, *ApJ*, 758, 56
- Shkolnik, E. L., & Barman, T. S. 2014, *AJ*, 148, 64
- Shkolnik, E. L., Rolph, K. A., Peacock, S., & Barman, T. S. 2014, *ApJL*, 796, L20
- Shkolnik, E. L., Allers, K. N., Kraus, A. L., Liu, M. C., & Flagg, L. 2017, *AJ*, 154, 69
- Short, C. I., & Hauschildt, P. H. 2005, *ApJ*, 618, 926
- Song, I., Zuckerman, B., & Bessell, M. S. 2003, *ApJ*, 599, 342
- Stassun, K. G., Oelkers, R. J., Pepper, J., et al. 2017, arXiv:1706.00495
- Stelzer, B., Marino, A., Micela, G., López-Santiago, J., & Liefke, C. 2013, *MNRAS*, 431, 2063
- Stelzer, B., Damasso, M., Scholz, A., & Matt, S. P. 2016, *MNRAS*, 463, 1844
- Sterzik, M. F., Alcalá, J. M., Covino, E., & Petr, M. G. 1999, *A&A*, 346, L41
- Stock, J., & Wroblewski, H. 1972, *A&A*, 18, 341
- Szczygieł, D. M., Socrates, A., Paczyński, B., Pojmański, G., & Pilecki, B. 2008, *AcA*, 58, 405
- Tian, F. 2009, *ApJ*, 703, 905
- Tian, F., France, K., Linsky, J. L., Mauas, P. J. D., & Veytes, M. C. 2014, *Earth and Planetary Science Letters*, 385, 22
- Tian, F., & Ida, S. 2015, *Nature Geoscience*, 8, 177
- Tokunaga, A. T., & Vacca, W. D. 2005, *PASP*, 117, 421
- Torres, C. A. O., da Silva, L., Quast, G. R., de la Reza, R., & Jilinski, E. 2000, *AJ*, 120, 1410
- Torres, C. A. O., Quast, G. R., Melo, C. H. F., & Sterzik, M. F. 2008, *Handbook of Star Forming Regions*, Volume II, 5, 757
- Upgren, A. R., Weis, E. W., & Hanson, R. B. 1985, *AJ*, 90, 2039
- van Altena, W. F. 1966, *AJ*, 71, 482
- van Leeuwen, F. 2009, *A&A*, 497, 209
- van Rhijn, P. J., & Raimond, J. J. 1934, *MNRAS*, 94, 508
- Ward-Duong, K., Patience, J., De Rosa, R. J., et al. 2015, *MNRAS*, 449, 2618
- Webb, R. A., Zuckerman, B., Platais, I., et al. 1999, *ApJL*, 512, L63
- Weinberger, A. J., Anglada-Escudé, G., & Boss, A. P. 2013, *ApJ*, 762, 118
- Weis, E. W., Deluca, E. E., & Upgren, A. R. 1979, *PASP*, 91, 766
- Weiss, E. W., & Upgren, A. R. 1982, *PASP*, 94, 475
- Weis, E. W., & Hanson, R. B. 1988, *AJ*, 96, 148
- West, A. A., Morgan, D. P., Bochanski, J. J., et al. 2011, *AJ*, 141, 97
- West, A. A., Weisenburger, K. L., Irwin, J., et al. 2015, *ApJ*, 812, 3
- Youngblood, A., France, K., Parke Loyd, R. O., et al. 2017, *ApJ*, 843, 31

Zuckerman, B., Webb, R. A., Schwartz, M., & Becklin,
E. E. 2001, ApJL, 549, L233

Zuckerman, B., Song, I., & Bessell, M. S. 2004, ApJL, 613,
L65
Zuckerman, B., & Song, I. 2004, ARA&A, 42, 685

Table 5. Target Sample *GALEX* Photometry

2MASS Designation	Disc. ^a	Spec.	<i>J</i>	FUV ^b	NUV ^b	<i>f</i> _{FUV} / <i>f</i> _J	<i>f</i> _{NUV} / <i>f</i> _J	Binary?	Binary Ref
Ref	Type	(mag)	(mag)	(mag)	(mag)				
TW Hya									
10120908–3124451	1	M4.0	8.848 ± 0.018	21.646 ± 0.318	20.234 ± 0.122	1.73e-05	6.36e-05	VB (1'') ^c	25
10284580–2830374	2	M5.0	10.953 ± 0.027	>22.577	22.325 ± 0.397	<5.10e-05	6.44e-05		
11091380–3001398	3	M1.5	7.629 ± 0.030	20.099 ± 0.138	18.037 ± 0.035	2.34e-05	1.56e-04	VB (0'')	7
11102788–3731520	3	M4.0	7.651 ± 0.019	17.720 ± 0.072	16.563 ± 0.024	2.14e-04	6.21e-04	SB, VB (1'')	3, 57
11210549–3845163	4	M2.0	8.999 ± 0.034	20.962 ± 0.425	19.255 ± 0.036	3.74e-05	1.80e-04		
11211723–3446454	4	M1.0	8.431 ± 0.043	19.643 ± 0.153	17.711 ± 0.043	7.46e-05	4.42e-04	VB (5'')	58
11315526–3436272	3	M2.0	7.669 ± 0.026	19.213 ± 0.111	17.446 ± 0.009	5.50e-05	2.80e-04	VB (0'1, 2'0)	59, 60
11321822–3018316	5	M4.0	15.350 ± 0.047	>21.780	>22.819	<6.10e-03	<2.34e-03	VB (80'')	5
11321831–3019518	6	M5.0	9.641 ± 0.024	>21.787	22.485 ± 0.409	<3.16e-05	1.66e-05	VB (80'')	5
11324124–2651559	7	M3.0	8.337 ± 0.024	19.953 ± 0.132	18.105 ± 0.023	5.14e-05	2.82e-04	VB (13'')	61
11393382–3040002	2	M4.5	9.985 ± 0.021	...	20.923 ± 0.282	...	9.60e-05		
11592786–4510192	8	M4.5	9.934 ± 0.024	>21.524	20.102 ± 0.168	<5.27e-05	1.95e-04		
12002750–3405371	9	M4.5	9.606 ± 0.024	22.189 ± 0.421	20.203 ± 0.114	2.11e-05	1.31e-04		
12023799–3328402	10	M5.0	10.686 ± 0.023	>22.161	21.711 ± 0.341	<5.86e-05	8.86e-05		
12072738–3247002	11	M3.0	8.618 ± 0.029	21.343 ± 0.408	19.754 ± 0.080	1.85e-05	8.00e-05	SB2	12
12153072–3948426	11	M0.0	8.166 ± 0.034	...	18.483 ± 0.063	...	1.70e-04		
12173920–3734433	10	M5.0	11.572 ± 0.024	>21.804	>22.339	<1.84e-04	<1.12e-04		
12265135–3316124	12	M5.0	10.691 ± 0.024	20.069 ± 0.296	19.032 ± 0.054	4.04e-04	1.05e-03	VB (0'')	12
12313807–4558593	13	M3.0	9.331 ± 0.030	>21.757	20.068 ± 0.166	<2.44e-05	1.16e-04	SB	62
12343629–4558075	14	M2.0	8.994 ± 0.026	20.830 ± 0.289	19.443 ± 0.083	4.20e-05	1.51e-04	VB (0'')	14
12350424–4136385	7	M2.0	9.122 ± 0.024	21.501 ± 0.468	19.741 ± 0.129	2.55e-05	1.29e-04		
12354615–4115531	8	M3.0	10.068 ± 0.027	>21.341	20.865 ± 0.263	<7.05e-05	1.09e-04		
<i>β Pic</i>									
0016496+4515417	15	M4.5	10.729 ± 0.025	>22.111	21.090 ± 0.088	<6.38e-05	1.63e-04	VB (30'')	63
0017353–6645124	16	M2.5	8.563 ± 0.021	21.041 ± 0.335	19.124 ± 0.081	2.33e-05	1.36e-04		
00193931+1951050	15	M4.5	10.926 ± 0.020	>22.995	>21.320	<3.39e-05	<1.58e-04	VB (53'')	15
00194303+1951117	15	M4.5	10.718 ± 0.020	...	21.249 ± 0.123	...	1.40e-04	VB (53'')	15

Table 5 continued

Table 5 (*continued*)

2MASS Designation	Disc. ^a	Spec.	<i>J</i>	FUV ^b	NUV ^b	<i>f</i> _{FUV} / <i>f</i> _J	<i>f</i> _{NUV} / <i>f</i> _J	Binary?	Binary Ref
Ref	Type	(mag)	(mag)	(mag)	(mag)				
00233468+2014282	17	K7.5	8.138 ± 0.020	...	18.182 ± 0.059	...	2.19e-04	VB (1.7")	18
00275023–3233060	18	M3.5	8.882 ± 0.032	21.067 ± 0.140	19.392 ± 0.034	3.04e-05	1.42e-04	VB (17.8")	64
00275035–3233238	18	M3.5	8.973 ± 0.027	20.361 ± 0.099	18.810 ± 0.027	6.35e-05	2.65e-04	VB (17.8")	64
00281434–3227556	15	M4.5	10.121 ± 0.022	22.425 ± 0.339	20.848 ± 0.109	2.73e-05	1.17e-04	VB (0.6")	18
00482667–1847204	15	M4.5	10.745 ± 0.023	>22.708	22.233 ± 0.268	<3.73e-05	5.78e-05		
00501752+0837341	15	M4.0	9.745 ± 0.023	>22.245	20.129 ± 0.174	<2.28e-05	1.60e-04	SB2	15
01071194–1935359	19	M0.5	8.149 ± 0.020	20.339 ± 0.196	18.461 ± 0.055	3.03e-05	1.71e-04	VB (0.4")	65
01132817–3821024	18	M0.0	8.487 ± 0.021	19.874 ± 0.158	18.354 ± 0.043	6.35e-05	2.57e-04	SB2, VB (1.3")	66, 67
01351393–0712517	20	M4.0	8.964 ± 0.021	>20.609	19.137 ± 0.049	<5.01e-05	1.94e-04	SB2	18
01354915–0753470	21	M4.0	10.667 ± 0.023	>22.741	22.134 ± 0.461	<3.37e-05	5.90e-05		
01365516–0647379	18	M4.0	9.707 ± 0.022	21.852 ± 0.036	20.375 ± 0.013	3.16e-05	1.23e-04	VB (5.6")	65
01535076–1459503	18	M3.0	7.938 ± 0.027	19.879 ± 0.121	18.122 ± 0.033	3.81e-05	1.92e-04	VB (2.9")	65
02175601+1225266	20	M4.0	9.963 ± 0.023	21.585 ± 0.122	19.955 ± 0.035	5.11e-05	2.29e-04		
02232663+2244069	22	M3.0	8.182 ± 0.018	19.472 ± 0.156	17.765 ± 0.041	6.94e-05	3.35e-04		
02272804+3058405	11	M2.0	8.817 ± 0.043	21.006 ± 0.194	18.980 ± 0.050	3.03e-05	1.96e-04	VB (22.1")	68
02282694+0218331	10	M5.0	12.124 ± 0.027	>22.330	>22.396	<1.88e-04	<1.77e-04		
02335984–1811525	15	M3.0	10.093 ± 0.029	21.688 ± 0.441	20.466 ± 0.175	5.24e-05	1.62e-04	VB (0.9")	65
02365171–5203036	23	M2.0	8.420 ± 0.023	20.487 ± 0.185	18.379 ± 0.038	3.39e-05	2.36e-04		
02450826–0708120	15	M4.0	10.786 ± 0.024	>23.273	21.439 ± 0.064	<2.31e-05	1.25e-04		
02485260–3404246	15	M4.0	9.308 ± 0.026	>20.992	18.290 ± 0.013	<4.83e-05	5.82e-04	SB1	18
03255277–3601161	15	M4.5	11.461 ± 0.023	...	21.622 ± 0.407	...	1.96e-04		
03323578+2843554	18	M4.0	9.357 ± 0.021	>21.817	20.464 ± 0.068	<2.36e-05	8.22e-05	VB (0.1, 0.5")	69
03393700+4531160	15	M3.5	9.948 ± 0.020	...	20.634 ± 0.280	...	1.21e-04		
04435686+3723033	22	M3.0	9.711 ± 0.022	>22.096	19.192 ± 0.022	<2.53e-05	3.67e-04	VB (9")	22
04480085+1439583	24	M5.0	11.679 ± 0.022	>19.979	19.961 ± 0.044	<1.09e-03	1.11e-03	VB (25.9")	24
04480258+1439516	24	M5.0	11.680 ± 0.022	>19.975	19.581 ± 0.076	<1.10e-03	1.57e-03	VB (25.9")	24
05004714–5715255	14	M0.5	7.095 ± 0.021	19.486 ± 0.120	17.511 ± 0.028	2.52e-05	1.55e-04		
05015881+0958587	11	M4.0	7.212 ± 0.023	18.069 ± 0.074	16.504 ± 0.020	1.03e-04	4.37e-04	SB2, VB (0.6")	70
05241914–1601153	16	M5.0	8.668 ± 0.027	20.197 ± 0.211	18.880 ± 0.081	5.57e-05	1.87e-04	VB (0.6")	65
05294468–3239141	25	M4.5	9.215 ± 0.026	21.716 ± 0.319	20.072 ± 0.094	2.27e-05	1.03e-04		
06131330–2742054	16	M3.5	8.002 ± 0.034	20.313 ± 0.171	18.706 ± 0.050	2.71e-05	1.19e-04	VB (0.1")	25

Table 5 *continued*

Table 5 (*continued*)

2MASS Designation	Disc. ^a	Spec.	<i>J</i>	FUV ^b	NUV ^b	<i>f</i> _{FUV} / <i>f</i> _J	<i>f</i> _{NUV} / <i>f</i> _J	Binary?	Binary Ref
Ref	Type	(mag)	(mag)	(mag)	(mag)				
08173943–8243298	18	M4.0	7.469 ± 0.023	...	17.670 ± 0.014	...	1.89e-04		
09361593+3731456	26	M2.0	8.085 ± 0.018	20.939 ± 0.189	18.920 ± 0.042	1.64e-05	1.06e-04	SB2	18
10141918+2104297	20	M0.5	7.074 ± 0.023	19.160 ± 0.172	17.343 ± 0.038	3.33e-05	1.78e-04	SB1	34
11493184–7851011	16	M1.0	9.449 ± 0.022	20.571 ± 0.214	19.064 ± 0.062	8.10e-05	3.25e-04		
14141700–1521125	21	M3.5	9.687 ± 0.024	>22.011	19.667 ± 0.090	<2.68e-05	2.32e-04	VB (1'':3, 64'':3)	64
15063505–3639297	15	M5.0	12.032 ± 0.023	>21.723	>21.828	<3.03e-04	<2.75e-04		
16430128–1754274	19	M0.5	9.443 ± 0.025	>20.466	19.349 ± 0.078	<8.88e-05	2.48e-04		
17173128–6657055	14	M4.5	8.542 ± 0.027	...	>22.256	...	<7.45e-06	VB (34'':0)	71
18011345+0948379	15	M4.0	10.294 ± 0.024	20.813 ± 0.202	20.354 ± 0.097	1.41e-04	2.15e-04		
18055491–5704307	15	M3.5	9.564 ± 0.024	>20.999	19.277 ± 0.044	<6.07e-05	2.97e-04		
18420483–5554126	21	M4.5	10.677 ± 0.023	>22.343	21.113 ± 0.289	<4.91e-05	1.52e-04		
18420694–5554254	16	M3.5	9.488 ± 0.024	>22.367	19.701 ± 0.105	<1.61e-05	1.87e-04		
19102820–2319486	18	M4.0	9.101 ± 0.021	...	19.076 ± 0.111	...	2.33e-04		
19243494–3442392	18	M4.0	9.670 ± 0.023	>22.559	19.528 ± 0.033	<1.59e-05	2.60e-04		
19260075–5331269	15	M4.0	9.595 ± 0.027	>22.276	20.806 ± 0.186	<1.93e-05	7.47e-05	SB2	15
19560294–32207186	17	M4.0	8.959 ± 0.027	21.126 ± 0.188	19.503 ± 0.055	3.09e-05	1.38e-04	SB2, VB (26'':3)	72
19560438–32207376	17	M0.0	8.710 ± 0.029	20.963 ± 0.169	19.162 ± 0.044	2.86e-05	1.50e-04	VB (26'':3)	72
20013718–3313139	19	M1.0	9.155 ± 0.024	21.111 ± 0.230	19.334 ± 0.071	3.76e-05	1.93e-04		
20083784–2545256	15	M4.5	10.899 ± 0.024	>22.143	21.242 ± 0.180	<7.24e-05	1.66e-04		
20085368–3519486	15	M3.5	9.170 ± 0.026	21.454 ± 0.395	20.098 ± 0.129	2.78e-05	9.69e-05		
20100002–2801410	16	M2.5	8.651 ± 0.023	19.725 ± 0.078	18.427 ± 0.028	8.47e-05	2.80e-04	SB2, VB (0'':6)	18, 65
20333759–2556521	16	M4.5	9.712 ± 0.024	>22.719	20.249 ± 0.091	<1.43e-05	1.39e-04		
20415111–3226073	27	M4.5	5.807 ± 0.026	17.541 ± 0.033	15.927 ± 0.007	4.61e-05	2.04e-04	VB (2'':3)	64
20450949–3120266	27	M1.0	5.436 ± 0.017	17.437 ± 0.038	15.614 ± 0.010	3.61e-05	1.93e-04		
21100535–1919573	16	M2.0	8.112 ± 0.030	20.335 ± 0.171	18.581 ± 0.052	2.94e-05	1.48e-04		
21103096–2710513	28	M5.0	11.200 ± 0.026	>22.480	21.023 ± 0.118	<7.01e-05	2.68e-04	VB (9'':5)	65
21103147–2710578	18	M4.5	10.296 ± 0.023	>22.480	20.903 ± 0.125	<3.05e-05	1.30e-04	VB (9'':5)	65
21200779–1645475	15	M4.5	10.149 ± 0.022	>22.671	20.981 ± 0.175	<2.23e-05	1.06e-04		
21374019+0137137	26	M5.0	8.802 ± 0.020	20.397 ± 0.042	18.737 ± 0.013	5.24e-05	2.42e-04	VB (0'':4)	73
21384755+0504518	15	M4.0	10.721 ± 0.023	>22.922	21.585 ± 0.085	<3.00e-05	1.03e-04	SB3	15
22004158+2715135	17	M0.0	8.556 ± 0.034	...	18.032 ± 0.032	...	3.69e-04		

Table 5 *continued*

Table 5 (*continued*)

2MASS Designation	Disc. ^a	Spec.	<i>J</i> (mag)	FUV ^b (mag)	NUV ^b (mag)	<i>f</i> _{FUV} / <i>f</i> _J	<i>f</i> _{NUV} / <i>f</i> _J	Binary?	Binary Ref
	Ref	Type							
22085034+1144131	15	M4.5	9.901 ± 0.023	>22.213	20.454 ± 0.032	<2.71e-05	1.37e-04		
22445794–3315015	11	M4.0	7.786 ± 0.019	20.307 ± 0.141	...	2.24e-05	...	VB (35'')	64
22450004–3315258	11	M4.5	8.681 ± 0.020	20.716 ± 0.175	...	3.49e-05	...	VB (35'')	64
23172807+1936469	16	M3.5	8.020 ± 0.024	20.006 ± 0.134	18.673 ± 0.046	3.66e-05	1.25e-04		
23314492–0244395	28	M4.5	9.507 ± 0.023	16.501 ± 0.007	15.613 ± 0.003	3.63e-03	8.23e-03	VB (146'')	28
23323085–1215513	29	M0.0	7.450 ± 0.021	19.841 ± 0.016	17.775 ± 0.005	2.52e-05	1.69e-04		
23353085–1908389	10	M5.0	11.513 ± 0.022	>23.189	23.250 ± 0.564	<4.87e-05	4.60e-05		
23500639+2659519	16	M3.5	10.142 ± 0.020	21.705 ± 0.283	20.138 ± 0.092	5.40e-05	2.29e-04		
23512227+2344207	16	M4.0	9.683 ± 0.023	22.067 ± 0.452	20.083 ± 0.061	2.53e-05	1.58e-04		
Tuc-Hor									
00125703–7952073	30	M3.0	9.682 ± 0.026	...	19.858 ± 0.107	...	1.94e-04		
00144767–6003477	30	M3.5	9.708 ± 0.021	20.964 ± 0.224	19.233 ± 0.063	7.16e-05	3.53e-04		
00152752–6414545	30	M2.0	9.325 ± 0.025	21.453 ± 0.373	19.805 ± 0.113	3.21e-05	1.46e-04		
00235732–5331435	30	M4.0	11.112 ± 0.023	>22.400	21.511 ± 0.207	<6.96e-05	1.58e-04		
00273330–6157169	30	M4.0	10.327 ± 0.026	>22.085	20.819 ± 0.215	<4.51e-05	1.45e-04		
00284683–6751446	30	M4.5	11.399 ± 0.027	>21.895	22.472 ± 0.492	<1.44e-04	8.48e-05		
00332438–5116433	30	M3.5	9.861 ± 0.023	22.563 ± 0.469	20.723 ± 0.146	1.89e-05	1.03e-04		
00395579–3816584	30	M1.5	8.777 ± 0.021	20.421 ± 0.172	18.494 ± 0.045	5.01e-05	2.96e-04		
00394063–6224125	30	M5.0	11.233 ± 0.023	>22.361	21.873 ± 0.298	<8.06e-05	1.26e-04		
00421010–5444431	30	M3.0	9.814 ± 0.024	21.447 ± 0.221	20.191 ± 0.070	5.06e-05	1.61e-04		
00425349–6117384	30	M4.0	11.289 ± 0.022	>21.934	>22.306	<1.26e-04	<8.92e-05		
00485254–6526330	30	M3.0	10.407 ± 0.023	>22.216	21.305 ± 0.133	<4.30e-05	9.96e-05		
00493566–6347416	30	M1.5	9.281 ± 0.029	21.428 ± 0.222	19.611 ± 0.056	3.15e-05	1.68e-04		
00514081–5913320	30	M4.5	11.277 ± 0.022	>22.688	22.820 ± 0.372	<6.21e-05	5.50e-05	VB (11'')	74
01024375–6235344	30	M3.0	9.642 ± 0.023	>22.505	20.824 ± 0.124	<1.63e-05	7.67e-05	VB (0'')	74
01033563–5515561	31	M5.0	10.162 ± 0.023	...	20.224 ± 0.135	...	2.15e-04	VB (0'')	31
01071194–1935359	19	M1.0	8.149 ± 0.020	20.339 ± 0.196	18.461 ± 0.055	3.03e-05	1.71e-04		
01160045–6747311	30	M4.0	11.776 ± 0.023	>22.740	22.490 ± 0.378	<9.38e-05	1.18e-04		
01180670–6258591	30	M5.0	11.530 ± 0.026	>22.206	22.205 ± 0.370	<1.22e-04	1.22e-04		
01211297–6117281	30	M4.0	11.308 ± 0.026	>21.691	21.380 ± 0.376	<1.60e-04	2.13e-04		
01224511–6318446	30	M3.5	9.833 ± 0.021	21.534 ± 0.375	20.095 ± 0.114	4.75e-05	1.79e-04		

Table 5 *continued*

Table 5 (*continued*)

2MASS Designation	Disc. ^a	Spec.	<i>J</i>	FUV ^b	NUV ^b	<i>f</i> _{FUV} / <i>f</i> _J	<i>f</i> _{NUV} / <i>f</i> _J	Binary?	Binary Ref
Ref	Type	(mag)	(mag)	(mag)	(mag)				
01233280–4113110	30	M4.0	10.796 ± 0.027	>21.759	21.424 ± 0.078	<9.39e-05	1.28e-04		
01253196–6646023	30	M4.0	10.946 ± 0.024	>22.925	21.393 ± 0.312	<3.68e-05	1.51e-04		
01275875–6032243	32	M4.0	11.079 ± 0.023	>22.787	21.635 ± 0.220	<4.72e-05	1.36e-04		
01283025–4921094	30	M4.0	10.561 ± 0.024	>22.643	20.870 ± 0.065	<3.35e-05	1.71e-04		
01372781–4558261	30	M5.0	11.106 ± 0.024	>23.237	22.760 ± 0.315	<3.20e-05	4.96e-05	VB (0'')	74
01505688–5844032	32	M3.0	9.540 ± 0.024	21.346 ± 0.283	19.768 ± 0.091	4.32e-05	1.85e-04		
01521830–5950168	19	M1.5	8.941 ± 0.019	20.480 ± 0.125	19.146 ± 0.042	5.52e-05	1.89e-04		
01532494–6833226	32	M4.5	11.070 ± 0.026	>22.371	21.532 ± 0.137	<6.87e-05	1.49e-04		
02001277–0840516	16	M2.0	8.766 ± 0.024	20.604 ± 0.048	19.046 ± 0.019	4.19e-05	1.76e-04		
02001992–6614017	32	M4.0	10.741 ± 0.024	22.292 ± 0.493	21.312 ± 0.138	5.46e-05	1.35e-04		
02045317–5346162	16	M4.0	10.438 ± 0.024	>22.833	21.295 ± 0.216	<2.51e-05	1.03e-04		
02070176–4406380	32	M2.0	9.270 ± 0.027	21.425 ± 0.173	20.009 ± 0.033	3.13e-05	1.15e-04	SB1, VB (6'')	18, 69
02125819–5851182	32	M2.0	9.325 ± 0.024	20.480 ± 0.250	19.249 ± 0.074	7.86e-05	2.44e-04		
02180960–6657524	30	M4.5	10.819 ± 0.022	>23.112	22.766 ± 0.296	<2.76e-05	3.79e-05	VB (0'')	74
02192210–3925225	30	M5.0	11.381 ± 0.026	>22.257	>22.370	<1.02e-04	<9.16e-05		
02205139–5823411	32	M3.0	9.666 ± 0.022	21.546 ± 0.298	19.876 ± 0.082	4.03e-05	1.88e-04		
02242453–7033211	30	M3.5	10.374 ± 0.021	>22.792	20.922 ± 0.085	<2.46e-05	1.37e-04		
02294569–5541496	30	M5.0	11.103 ± 0.023	>23.052	>22.941	<3.79e-05	<4.19e-05		
02321934–5746117	32	M4.0	11.099 ± 0.026	>22.066	21.710 ± 0.289	<9.35e-05	1.30e-04		
02341866–5128462	30	M4.5	10.626 ± 0.024	22.439 ± 0.438	21.485 ± 0.231	4.29e-05	1.03e-04		
02383255–7528065	30	M4.0	11.670 ± 0.023	>22.818	22.285 ± 0.198	<7.91e-05	1.29e-04		
02414730–5259306	33	M2.0	8.481 ± 0.027	20.318 ± 0.144	18.687 ± 0.047	4.19e-05	1.88e-04	VB (0'')	75
02420204–5359147	32	M4.5	10.833 ± 0.022	>22.073	21.427 ± 0.308	<7.27e-05	1.32e-04	VB (23'')	72
02420404–5359000	32	M4.5	10.110 ± 0.023	20.783 ± 0.261	20.011 ± 0.141	1.23e-04	2.50e-04	VB (23'')	72
02474639–5804272	32	M2.0	9.356 ± 0.024	21.819 ± 0.359	19.660 ± 0.080	2.36e-05	1.72e-04		
02502222–6545552	32	M3.0	10.304 ± 0.024	21.904 ± 0.357	20.732 ± 0.104	5.22e-05	1.54e-04		
02503959–3409050	32	M3.5	10.479 ± 0.027	>21.809	20.951 ± 0.075	<6.69e-05	1.47e-04		
02523550–7831183	30	M4.5	11.670 ± 0.023	>21.729	>22.248	<2.16e-04	<1.34e-04		
02543316–5108313	33	M1.0	8.668 ± 0.027	20.646 ± 0.180	19.192 ± 0.064	3.68e-05	1.41e-04		
02553178–5702522	32	M4.5	11.074 ± 0.021	22.246 ± 0.295	21.032 ± 0.130	7.74e-05	2.37e-04		
02590284–6120000	30	M4.0	11.598 ± 0.024	>22.939	22.246 ± 0.356	<6.62e-05	1.25e-04		

Table 5 *continued*

Table 5 (*continued*)

2MASS Designation	Disc. ^a	Spec.	<i>J</i>	FUV ^b	NUV ^b	<i>f</i> _{FUV} / <i>f</i> _J	<i>f</i> _{NUV} / <i>f</i> _J	Binary?	Binary Ref
Ref	Type	(mag)	(mag)	(mag)	(mag)				
02591904–5122341	30	M5.5	11.685 ± 0.020	22.506 ± 0.343	22.220 ± 0.203	1.07e-04	1.39e-04		
03050556–5317182	32	M4.5	11.135 ± 0.023	>23.093	21.785 ± 0.251	<3.75e-05	1.25e-04		
03050976–3725058	16	M1.5	9.544 ± 0.022	21.484 ± 0.270	19.710 ± 0.088	3.82e-05	1.96e-04	VB (0'')	65
03083950–3844363	32	M4.5	11.249 ± 0.023	>22.709	22.130 ± 0.305	<5.94e-05	1.01e-04		
03104941–3616471	32	M4.0	10.629 ± 0.023	21.061 ± 0.266	20.510 ± 0.131	1.53e-04	2.54e-04		
03114544–4719501	32	M3.0	10.437 ± 0.023	>22.773	21.705 ± 0.273	<2.65e-05	7.08e-05		
03210395–6816475	30	M4.0	10.356 ± 0.039	21.531 ± 0.308	20.642 ± 0.117	7.72e-05	1.75e-04		
03244056–3904227	32	M3.5	9.870 ± 0.023	20.394 ± 0.166	18.887 ± 0.052	1.41e-04	5.63e-04		
03291649–3702502	32	M4.0	10.649 ± 0.026	22.494 ± 0.472	21.338 ± 0.181	4.16e-05	1.21e-04		
03512287–5154582	32	M4.0	10.608 ± 0.022	>22.118	>22.415	<5.67e-05	<4.31e-05	VB (0'')	74
03561624–3915219	32	M4.0	10.460 ± 0.021	>21.622	20.080 ± 0.106	<7.81e-05	3.23e-04		
04074372–6895111	30	M3.0	10.407 ± 0.021	21.204 ± 0.246	19.909 ± 0.044	1.09e-04	3.60e-04		
04133314–5231586	30	M2.5	10.003 ± 0.026	...	22.376 ± 0.498	...	2.56e-05		
04133609–4413325	32	M3.5	10.769 ± 0.024	>22.027	21.158 ± 0.279	<7.15e-05	1.59e-04		
04213904–7233562	16	M2.0	9.870 ± 0.022	>21.642	20.396 ± 0.126	<4.45e-05	1.40e-04		
04274963–3327010	30	M4.0	11.210 ± 0.023	>22.592	22.511 ± 0.586	<6.38e-05	6.87e-05		
04365738–1613065	16	M3.5	9.117 ± 0.026	20.051 ± 0.142	18.773 ± 0.049	9.63e-05	3.13e-04		
04440099–6624036	16	M0.0	9.474 ± 0.024	21.227 ± 0.127	19.715 ± 0.032	4.53e-05	1.83e-04		
04470041–5134405	30	M2.0	10.062 ± 0.022	22.264 ± 0.402	21.054 ± 0.191	3.00e-05	9.14e-05		
04475779–5035200	30	M4.0	10.868 ± 0.024	21.669 ± 0.407	>22.329	1.09e-04	<5.93e-05	VB (0'')	74
04515303–4647309	30	K8.0	9.800 ± 0.024	>22.125	>22.325	<2.68e-05	<2.23e-05	SB	30
05111098–4903597	16	M3.0	10.641 ± 0.026	19.923 ± 0.199	19.374 ± 0.054	4.41e-04	7.32e-04	VB (2'')	74
05392505–4245211	16	M1.5	9.446 ± 0.021	21.777 ± 0.504	19.319 ± 0.091	2.66e-05	2.56e-04		
20143542–5430588	30	M4.0	10.372 ± 0.024	21.814 ± 0.416	21.079 ± 0.157	6.03e-05	1.19e-04		
20291446–5456116	30	M4.5	11.225 ± 0.024	>23.511	22.264 ± 0.347	<2.77e-05	8.75e-05		
20423672–5425263	30	M4.0	10.748 ± 0.023	21.679 ± 0.281	20.886 ± 0.126	9.66e-05	2.01e-04		
21083826–4244540	30	M4.5	10.135 ± 0.024	>21.988	>23.279	<4.13e-05	<1.26e-05		
21100614–5811483	30	M4.0	10.894 ± 0.023	>22.020	20.489 ± 0.183	<8.07e-05	3.31e-04		
21143354–4213528	30	M4.0	11.380 ± 0.024	>22.229	21.767 ± 0.194	<1.04e-04	1.59e-04		
21163528–6005124	30	M3.5	10.191 ± 0.023	20.794 ± 0.158	19.884 ± 0.058	1.31e-04	3.02e-04		
21275054–6841033	30	M4.0	10.424 ± 0.022	>22.081	21.202 ± 0.072	<4.95e-05	1.11e-04		

Table 5 *continued*

Table 5 (*continued*)

2MASS Designation	Disc. ^a	Spec.	<i>J</i>	FUV ^b	NUV ^b	<i>f</i> _{FUV} / <i>f</i> _J	<i>f</i> _{NUV} / <i>f</i> _J	Binary?	Binary Ref
Ref	Type	(mag)	(mag)	(mag)	(mag)				
21354554–4218343	30	M5.0	11.682 ± 0.021	22.661 ± 0.341	21.602 ± 0.155	9.24e-05	2.45e-04		
21370885–6036054	18	M3.0	9.644 ± 0.023	21.155 ± 0.222	19.577 ± 0.048	5.67e-05	2.42e-04		
21380269–5744583	30	M3.5	10.874 ± 0.026	>22.841	21.006 ± 0.133	<3.72e-05	2.02e-04		
21490499–6413039	16	M4.5	10.353 ± 0.024	22.361 ± 0.349	20.866 ± 0.074	3.58e-05	1.42e-04	VB (0'')	76
21504048–5113380	30	M3.5	10.342 ± 0.022	22.240 ± 0.492	21.212 ± 0.189	3.97e-05	1.02e-04		
22021626–4210329	16	M0.5	8.925 ± 0.026	20.768 ± 0.157	19.182 ± 0.042	4.17e-05	1.80e-04		
22025453–6440441	30	M2.0	9.055 ± 0.027	20.884 ± 0.192	19.208 ± 0.060	4.23e-05	1.98e-04		
22223966–6303258	30	M3.5	10.183 ± 0.024	22.135 ± 0.480	20.671 ± 0.113	3.77e-05	1.45e-04		
22244102–7724036	30	M4.0	11.417 ± 0.023	>23.019	21.696 ± 0.256	<5.21e-05	1.76e-04		
22444835–6650032	30	M5.0	11.030 ± 0.026	>22.997	22.165 ± 0.091	<3.72e-05	8.01e-05		
22463471–7353504	30	M2.5	9.664 ± 0.024	21.365 ± 0.180	19.754 ± 0.020	4.76e-05	2.10e-04		
23124644–5049240	30	M4.0	9.117 ± 0.022	21.389 ± 0.235	...	2.81e-05	...		
23130558–6127077	30	M4.5	10.932 ± 0.021	>22.175	22.328 ± 0.400	<7.25e-05	6.30e-05		
23131671–4933154	18	M3.5	9.763 ± 0.022	21.151 ± 0.221	19.615 ± 0.074	6.34e-05	2.61e-04		
23170011–7432095	30	M3.5	10.402 ± 0.024	>22.009	21.492 ± 0.215	<5.19e-05	8.34e-05		
23261069–7323498	29	K7.5	8.840 ± 0.029	20.018 ± 0.190	18.762 ± 0.070	7.70e-05	2.45e-04		
23273447–8512364	30	M4.0	10.850 ± 0.022	>22.526	20.944 ± 0.123	<4.86e-05	2.09e-04		
23285763–6802338	16	M2.5	9.257 ± 0.023	20.479 ± 0.151	19.124 ± 0.035	7.39e-05	2.57e-04		
23291752–6749598	30	M3.5	10.793 ± 0.025	22.360 ± 0.385	21.198 ± 0.122	5.38e-05	1.57e-04		
23382851–6749025	30	M4.0	10.909 ± 0.027	20.661 ± 0.172	19.971 ± 0.066	2.86e-04	5.40e-04		
23424333–6224564	30	M4.5	11.298 ± 0.026	>22.025	20.732 ± 0.223	<1.17e-04	3.67e-04		
23452225–7126505	16	M3.5	10.194 ± 0.024	22.081 ± 0.360	20.262 ± 0.116	4.00e-05	2.14e-04		
23474694–6517249	16	M1.0	9.099 ± 0.024	21.135 ± 0.338	19.274 ± 0.085	3.49e-05	1.94e-04		
23524562–5229593	30	M4.5	11.574 ± 0.023	>23.977	22.321 ± 0.137	<2.49e-05	1.14e-04		
23570417–0337559	30	M3.0	10.895 ± 0.022	22.684 ± 0.266	21.466 ± 0.101	4.39e-05	1.35e-04	VB (0'')	69
AB Dor									
00020382+0408129	9	M3.0	10.402 ± 0.042	>25.265	>24.077	<2.59e-06	<7.72e-06		
00192626+4614078	26	M8.0	12.603 ± 0.021	>22.555	>22.555	<2.38e-04	<2.38e-04		
00485822+4435091	26	M4.0	9.125 ± 0.025	...	19.214 ± 0.078	...	2.10e-04	VB (1'')	77
01034013+4051288	26	M0.0	8.134 ± 0.019	19.392 ± 0.031	17.350 ± 0.008	7.15e-05	4.69e-04	VB (0'3, 26'0)	73, 64
01034210+4051158	34	M2.5	9.372 ± 0.038	21.477 ± 0.091	19.791 ± 0.091	3.28e-05	1.55e-04	VB (26'0)	64

Table 5 *continued*

Table 5 (*continued*)

2MASS Designation	Disc. ^a	Spec.	<i>J</i>	FUV ^b	NUV ^b	<i>f</i> _{FUV} / <i>f</i> _J	<i>f</i> _{NUV} / <i>f</i> _J	Binary?	Binary Ref
Ref	Type	(mag)	(mag)	(mag)	(mag)				
01035369–2805518	9	M4.0	11.661 ± 0.033	>24.031	22.445 ± 0.195	<2.57e-05	1.11e-04		
01225093–2439505	16	M3.5	10.084 ± 0.028	21.154 ± 0.289	20.673 ± 0.144	8.50e-05	1.32e-04	VB (1'':5)	78
01242767–3355086	34	M4.5	9.203 ± 0.036	20.301 ± 0.059	18.861 ± 0.017	8.29e-05	3.12e-04	VB (2'':0, 37'':0)	79, 64
01484087–4830519	16	M1.5	9.194 ± 0.027	21.250 ± 0.169	19.314 ± 0.030	3.43e-05	2.04e-04	VB (71'':9)	72
02030658–5545420	32	M4.5	11.302 ± 0.027	>22.293	21.338 ± 0.253	<9.14e-05	2.20e-04		
02070786–1810077	18	M4.0	10.698 ± 0.024	20.678 ± 0.190	19.709 ± 0.084	2.32e-04	5.66e-04		
02085359+4926565	34	M3.0	8.423 ± 0.023	20.487 ± 0.183	18.690 ± 0.020	3.40e-05	1.78e-04		
02105345–4603513	35	M4.0	11.228 ± 0.021	>22.889	21.020 ± 0.178	<4.93e-05	2.76e-04		
02523096–1548357	16	M2.5	10.543 ± 0.021	22.568 ± 0.161	20.833 ± 0.048	3.53e-05	1.74e-04		
02545247–0709255	16	M3.0	9.999 ± 0.025	22.386 ± 0.231	21.151 ± 0.065	2.53e-05	7.88e-05	VB (4'':1)	69
03100305–2341308	36	M3.5	9.413 ± 0.024	20.554 ± 0.246	19.508 ± 0.112	7.96e-05	2.09e-04		
03472333–0158195	37	M3.0	7.804 ± 0.026	...	18.551 ± 0.047	...	1.14e-04		
04084031–2705473	16	M3.0	10.813 ± 0.024	21.849 ± 0.357	20.884 ± 0.174	8.77e-05	2.13e-04		
04093930–2648489	16	M1.5	9.510 ± 0.027	21.325 ± 0.366	19.967 ± 0.127	4.28e-05	1.50e-04		
04141730–0906544	34	M4.5	9.630 ± 0.024	21.714 ± 0.474	20.541 ± 0.188	3.34e-05	9.84e-05		
04363294–7851021	16	M4.0	10.977 ± 0.023	>22.489	20.886 ± 0.168	<5.66e-05	2.48e-04		
04424932–1452268	16	M4.0	10.239 ± 0.027	>22.231	20.523 ± 0.176	<3.64e-05	1.75e-04		
04514615–2400087	16	M3.0	10.556 ± 0.026	>22.326	20.514 ± 0.113	<4.46e-05	2.37e-04		
04522441–1649219	22	M3.0	7.740 ± 0.021	19.382 ± 0.083	17.979 ± 0.026	5.02e-05	1.83e-04		
04554034–1917553	16	M0.5	9.778 ± 0.022	22.047 ± 0.271	19.363 ± 0.056	2.82e-05	3.34e-04		
05130132–7027418	16	M3.5	9.209 ± 0.026	...	20.763 ± 0.345	...	5.45e-05	VB (1'':7)	69
05240991–4223054	16	M0.5	10.583 ± 0.021	>21.710	20.814 ± 0.143	<8.07e-05	1.84e-04	VB (0'':2)	75
05254166–0909123	34	M4.0	8.454 ± 0.026	...	19.373 ± 0.113	...	9.77e-05		
05301858–5358483	16	M3.0	7.913 ± 0.021	20.065 ± 0.136	18.600 ± 0.032	3.14e-05	1.21e-04	VB (0'':2, 4'':3)	69
05531299–4505119	16	M0.5	8.596 ± 0.030	21.319 ± 0.443	>22.745	1.86e-05	<4.99e-06		
06022455–1634494	16	M0.0	8.991 ± 0.026	21.107 ± 0.487	19.358 ± 0.120	3.24e-05	1.62e-04		
08034469+0827000	9	M6.0	11.831 ± 0.022	>23.023	>22.851	<7.60e-05	<8.91e-05		
08412991+6425032	38	M2.0	9.204 ± 0.020	21.404 ± 0.386	19.922 ± 0.135	3.00e-05	1.18e-04	VB (155'':7)	64
09321267+3358285	26	M3.5	9.895 ± 0.021	21.987 ± 0.428	20.402 ± 0.042	3.32e-05	1.43e-04		
09510459+3558098	34	M5.0	10.577 ± 0.021	>22.323	22.067 ± 0.407	<4.56e-05	5.78e-05	VB (13'':5)	(80)
10121768–0344441	16	M1.5	5.888 ± 0.021	20.828 ± 0.180	18.178 ± 0.036	2.41e-06	2.76e-05		

Table 5 *continued*

Table 5 (*continued*)

2MASS Designation	Disc. ^a	Spec.	<i>J</i>	FUV ^b	NUV ^b	<i>f</i> _{FUV} / <i>f</i> _J	<i>f</i> _{NUV} / <i>f</i> _J	Binary?	Binary Ref
Ref	Type	(mag)	(mag)	(mag)	(mag)				
1028555+0050275	39	M2.0	6.176 ± 0.021	21.301 ± 0.064	19.006 ± 0.012	2.03e-06	1.68e-05		
11254754–4410267	16	M4.0	10.341 ± 0.026	21.237 ± 0.289	20.658 ± 0.190	9.98e-05	1.70e-04	VB (0'')	69
12151838–0237283	16	M0.0	8.671 ± 0.034	20.943 ± 0.382	18.895 ± 0.091	2.81e-05	1.85e-04		
12383713–2703348	16	M2.5	8.728 ± 0.035	21.309 ± 0.093	19.401 ± 0.021	2.11e-05	1.23e-04	VB (0'')	73
12573935+3513194	34	M4.5	8.872 ± 0.035	20.504 ± 0.181	18.658 ± 0.049	5.06e-05	2.77e-04	VB (0'1, 16'')	73, 64
12574030+3513306	39	M0.0	7.401 ± 0.019	19.487 ± 0.112	17.700 ± 0.029	3.33e-05	1.73e-04	VB (0'2, 16'')	73, 64
13142039+1320011	26	M7.0	9.754 ± 0.022	>22.076	20.975 ± 0.229	<2.68e-05	7.40e-05	VB (0'1)	81
13350945+5039167	26	M3.0	9.308 ± 0.037	20.699 ± 0.033	18.980 ± 0.004	6.33e-05	3.08e-04		
14190331+6451463	16	M3.0	10.386 ± 0.020	21.857 ± 0.478	19.964 ± 0.125	5.88e-05	3.36e-04	VB (4'')	69
15594729+4403595	16	M1.0	8.509 ± 0.021	20.329 ± 0.227	18.615 ± 0.032	4.26e-05	2.07e-04	VB (5'')	69
16074132–1103073	16	M4.0	9.817 ± 0.023	20.402 ± 0.310	19.439 ± 0.094	1.33e-04	3.23e-04	VB (0'')	18
16232165+6149149	16	M2.5	10.055 ± 0.022	20.438 ± 0.220	18.609 ± 0.056	1.60e-04	7.94e-04		
16455062+0343014	26	M3.0	9.269 ± 0.021	20.454 ± 0.324	19.557 ± 0.064	7.65e-05	1.75e-04	VB (0'4)	69
17383964+6114160	37	M0.0	7.618 ± 0.024	18.756 ± 0.095	16.979 ± 0.028	7.98e-05	4.10e-04	VB (0'1, 8'')	82, 83
19420065–2104051	16	M3.5	8.692 ± 0.019	...	19.339 ± 0.078	...	1.26e-04	SB2	18
20220177–3653014	16	M4.5	10.713 ± 0.022	>22.123	21.550 ± 0.229	<6.21e-05	1.05e-04		
20465795–0259320	16	M0.0	9.122 ± 0.026	20.954 ± 0.196	19.127 ± 0.057	4.21e-05	2.27e-04		
21464282–8543046	16	M3.5	8.844 ± 0.023	20.251 ± 0.179	>22.552	6.23e-05	<7.49e-06		
21471964–4803166	16	M4.0	10.734 ± 0.022	22.393 ± 0.374	21.015 ± 0.192	4.94e-05	1.76e-04		
21521039+0537356	29	M2.5	8.248 ± 0.026	19.991 ± 0.168	...	4.57e-05	...		
23060482+6355339	37	M1.0	7.815 ± 0.023	...	17.867 ± 0.059	...	2.17e-04		
23115362–4508004	29	M3.0	9.724 ± 0.024	21.018 ± 0.178	>23.003	6.92e-05	<1.11e-05		
23353085–1908389	10	M5.0	11.513 ± 0.022	>23.134	23.250 ± 0.504	<5.12e-05	4.60e-05		
23513366+3127229	16	M2.0	9.821 ± 0.021	21.295 ± 0.255	19.970 ± 0.068	5.86e-05	1.99e-04	VB (2'4, 126'')	84, 73
23514340+3127045	21	M4.0	10.388 ± 0.021	21.335 ± 0.248	>22.855	9.52e-05	<2.35e-05	VB (126'')	73
23520507–1100435	10	M8.0	12.840 ± 0.022	>25.265	>24.077	<2.44e-05	<7.29e-05		
Hyades									
01532073+2326411	40	M0.0	9.300 ± 0.020	>22.038	21.230 ± 0.211	<1.83e-05	3.85e-05		
01533916+3219225	41	M5.5	12.772 ± 0.023	...	>23.633	...	<1.03e-04		
01564147+3028349	40	M4.5	11.917 ± 0.023	>22.704	22.155 ± 0.277	<1.10e-04	1.83e-04		
02032864+2134168	40	M5.5	11.661 ± 0.023	>23.009	22.823 ± 0.418	<6.58e-05	7.81e-05		

Table 5 *continued*

Table 5 (*continued*)

2MASS Designation	Disc. ^a	Spec.	<i>J</i>	FUV ^b	NUV ^b	<i>f</i> _{FUV} / <i>f</i> _J	<i>f</i> _{NUV} / <i>f</i> _J	Binary?	Binary Ref
Ref	Type	(mag)	(mag)	(mag)	(mag)				
02111362+2058223	40	M4.5	11.405 ± 0.021	...	>22.026	...	<1.29e-04		
02122889+2859448	40	M5.0	12.443 ± 0.023	>22.347	>22.733	<2.49e-04	<1.74e-04		
02135203–0330595	40	M4.5	11.693 ± 0.024	23.988 ± 0.161	23.126 ± 0.096	2.75e-05	6.08e-05		
02145660+0347100	40	M2.5	10.281 ± 0.027	>23.092	22.155 ± 0.367	<1.71e-05	4.05e-05		
02164742+0112454	40	M1.5	9.786 ± 0.027	22.314 ± 0.073	20.611 ± 0.030	2.22e-05	1.07e-04		
02254751+2435239	40	M4.0	11.384 ± 0.020	>22.080	20.755 ± 0.225	<1.20e-04	4.07e-04		
02260988+1227138	40	M3.5	11.392 ± 0.021	>22.401	22.001 ± 0.322	<8.99e-05	1.30e-04		
02342952+3613110	41	M5.0	12.461 ± 0.021	>22.250	>22.532	<2.77e-04	<2.13e-04		
02350321+4104418	40	M3.5	11.373 ± 0.020	>22.028	22.348 ± 0.536	<1.25e-04	9.28e-05		
02354955–0711214	41	M6.0	12.452 ± 0.029	>24.080	>23.867	<5.09e-05	<6.19e-05		
02385711+3512042	40	M4.0	11.621 ± 0.020	>21.685	>21.972	<2.15e-04	<1.65e-04		
02410948+3936117	40	M4.0	11.752 ± 0.018	>21.984	>22.062	<1.84e-04	<1.71e-04		
02412431+1728445	40	M0.0	9.665 ± 0.018	>21.705	>22.189	<3.48e-05	<2.23e-05		
02461252+0556261	41	M4.0	12.044 ± 0.022	>22.453	...	<1.56e-04	...		
02482042+2352191	40	M3.5	10.847 ± 0.021	>21.745	22.164 ± 0.308	<9.96e-05	6.77e-05		
02485115+3038373	40	M3.0	11.320 ± 0.021	>21.815	>22.381	<1.44e-04	<8.57e-05		
02564122+3522346	40	M2.5	9.817 ± 0.022	>22.601	21.552 ± 0.241	<1.75e-05	4.61e-05		
02581582+2228559	40	M3.5	12.062 ± 0.022	>21.549	>22.195	<3.65e-04	<2.02e-04		
02592910+0828148	41	M5.5	12.986 ± 0.024	...	21.931 ± 0.630	...	6.02e-04		
02594633+3855363	40	M3.5	10.411 ± 0.020	...	18.891 ± 0.085	...	9.24e-04	VB (0'')	85
03040207+0045512	41	M5.0	11.806 ± 0.026	22.876 ± 0.157	21.856 ± 0.066	8.50e-05	2.18e-04		
03050786+2742278	40	M5.0	11.609 ± 0.022	20.910 ± 0.411	>22.053	4.34e-04	<1.51e-04		
03055439+2708326	40	M5.0	12.202 ± 0.021	>21.720	>22.121	<3.55e-04	<2.45e-04		
03061500+1205548	40	M4.5	11.288 ± 0.020	>22.093	21.971 ± 0.564	<1.09e-04	1.21e-04		
03071634+1026382	40	M4.5	12.329 ± 0.021	>22.555	>22.543	<1.85e-04	<1.87e-04		
03104340+1338356	40	M1.5	9.973 ± 0.023	>22.131	21.608 ± 0.281	<3.12e-05	5.05e-05		
03135540+3205502	40	M3.5	11.389 ± 0.023	>22.113	21.745 ± 0.288	<1.17e-04	1.64e-04		
03153783+3724143	40	M1.5	9.317 ± 0.023	20.993 ± 0.414	19.441 ± 0.109	4.87e-05	2.03e-04	VB (6'')	73
03181774+3133117	40	M5.0	12.597 ± 0.019	>21.870	>22.496	<4.45e-04	<2.50e-04		
03223165+2858291	40	M3.0	10.823 ± 0.024	>21.571	20.637 ± 0.232	<1.14e-04	2.70e-04		
03234864+3935320	40	M5.0	12.552 ± 0.022	>22.108	>22.575	<3.43e-04	<2.23e-04		

Table 5 *continued*

Table 5 (*continued*)

2MASS Designation	Disc. ^a	Spec.	<i>J</i>	FUV ^b	NUV ^b	<i>f</i> _{FUV} / <i>f</i> _J	<i>f</i> _{NUV} / <i>f</i> _J	Binary?	Binary Ref
Ref	Type	(mag)	(mag)	(mag)	(mag)				
03243615+2150186	42	M3.5	11.290 ± 0.021	...	>21.982	...	<1.20e-04		
03250307−0308204	40	M3.0	10.060 ± 0.023	>22.315	21.896 ± 0.350	<2.85e-05	4.20e-05		
03251116+1300334	40	M4.5	11.844 ± 0.022	>21.253	>22.259	<3.93e-04	<1.55e-04		
03300506+2405281	41	M5.0	12.386 ± 0.023	>22.641	22.090 ± 0.455	<1.80e-04	2.99e-04		
03301038+2648593	40	M5.0	12.360 ± 0.020	>21.475	>22.087	<5.14e-04	<2.93e-04		
03341053+2204213	40	M4.5	11.355 ± 0.022	>22.427	22.108 ± 0.444	<8.49e-05	1.14e-04		
03373331+1751145	42	M0.0	9.100 ± 0.021	>21.883	20.656 ± 0.226	<1.75e-05	5.43e-05	VB (16.0')	64
03380713+0634256	40	M5.0	11.893 ± 0.022	>21.532	>22.149	<3.18e-04	<1.80e-04		
03390711+2025267	40	M3.5	10.567 ± 0.021	22.288 ± 0.525	21.376 ± 0.145	4.67e-05	1.08e-04		
03404581+1734477	41	M5.0	12.698 ± 0.021	>21.870	21.884 ± 0.491	<4.88e-04	4.82e-04		
03405493+1929474	41	M6.0	13.217 ± 0.022	...	>21.965	...	<7.22e-04		
03415547+1845359	42	M2.0	9.710 ± 0.021	>21.828	20.942 ± 0.224	<3.24e-05	7.32e-05		
03420441+1625183	40	M4.0	11.609 ± 0.021	>22.052	21.380 ± 0.329	<1.51e-04	2.81e-04		
03433551+2621311	40	M3.5	10.772 ± 0.019	>22.706	21.510 ± 0.031	<3.84e-05	1.15e-04		
03463952+1524170	40	M4.0	10.733 ± 0.021	>21.798	19.824 ± 0.113	<8.54e-05	5.26e-04		
03502795+0406455	40	M4.0	11.456 ± 0.021	>21.841	>22.170	<1.60e-04	<1.18e-04		
03505737+1818069	41	M6.0	12.967 ± 0.021	>21.956	>22.306	<5.78e-04	<4.19e-04		
03515674+4112167	41	M5.0	12.449 ± 0.021	...	>21.662	...	<4.70e-04		
03524271+2512260	40	M5.5	12.960 ± 0.026	...	20.861 ± 0.441	...	1.57e-03		
03535304+3421348	40	M2.5	11.313 ± 0.020	...	>21.653	...	<1.67e-04		
03543319+1618563	43	M4.0	9.960 ± 0.024	20.607 ± 0.220	19.100 ± 0.046	1.26e-04	5.03e-04		
03553690+2118482	44	M5.5	12.063 ± 0.024	>21.869	>22.469	<2.72e-04	<1.57e-04		
03555715+1825564	45	M2.5	10.230 ± 0.024	>22.073	>22.101	<4.17e-05	<4.07e-05		
03581414+2103041	40	M4.5	12.245 ± 0.020	>22.309	>22.626	<2.15e-04	<1.60e-04		
03585452+2513113	42	M2.0	10.357 ± 0.022	>21.963	22.310 ± 0.449	<5.19e-05	3.77e-05		
03591417+2202380	40	M1.5	9.538 ± 0.025	>21.983	21.643 ± 0.185	<2.40e-05	3.28e-05		
03591499+1639520	46	M4.0	11.269 ± 0.021	>21.725	20.881 ± 0.388	<1.50e-04	3.26e-04		
03592659+2323077	40	M4.0	11.518 ± 0.024	...	20.361 ± 0.215	...	6.61e-04		
03595180+2236135	40	M3.0	11.021 ± 0.023	>22.203	>22.535	<7.67e-05	<5.65e-05		
04022771−0709286	40	M4.5	11.846 ± 0.026	>22.311	>22.823	<1.48e-04	<9.26e-05		
04025310+1824262	46	M3.0	10.770 ± 0.018	21.448 ± 0.561	21.862 ± 0.190	1.22e-04	8.33e-05	SB	86

Table 5 *continued*

Table 5 (*continued*)

2MASS Designation	Disc. ^a	Spec.	<i>J</i>	FUV ^b	NUV ^b	<i>f</i> _{FUV} / <i>f</i> _J	<i>f</i> _{NUV} / <i>f</i> _J	Binary?	Binary Ref
Ref	Type	(mag)	(mag)	(mag)	(mag)				
04033378+4021433	40	M3.0	10.987 ± 0.021	...	21.545 ± 0.560	...	1.36e-04		
04041073+1548219	47	M5.5	12.779 ± 0.023	>22.015	>22.635	<4.61e-04	<2.60e-04		
04041279+1859445	47	M4.0	11.918 ± 0.021	...	22.388 ± 0.216	...	1.48e-04		
04042701+2024303	40	M3.5	11.210 ± 0.024	>22.206	20.632 ± 0.054	<9.10e-05	3.88e-04		
04045789+3936077	40	M5.0	12.616 ± 0.023	...	>21.583	...	<5.90e-04		
04050779+2917075	40	M4.5	11.863 ± 0.023	>22.551	>22.256	<1.21e-04	<1.59e-04		
04060221+1815033	48	M1.0	9.488 ± 0.021	21.686 ± 0.710	21.028 ± 0.123	3.01e-05	5.51e-05		
04062060+1901391	42	M3.5	11.341 ± 0.022	...	21.549 ± 0.336	...	1.88e-04		
04073233+2016510	49	M4.5	11.450 ± 0.020	>22.169	21.847 ± 0.215	<1.17e-04	1.58e-04		
04084015+2333257	50	K9.0	9.380 ± 0.026	>22.291	21.288 ± 0.212	<1.56e-05	3.93e-05		
04104079+1444007	47	M4.5	12.388 ± 0.023	>22.560	>22.747	<1.94e-04	<1.64e-04		
04105676+2729154	46	M3.0	10.594 ± 0.020	>22.041	21.823 ± 0.320	<6.01e-05	7.34e-05		
04110610+1855448	40	M3.5	11.145 ± 0.021	>22.065	21.469 ± 0.347	<9.76e-05	1.69e-04		
04112766+1559317	51	M3.0	10.807 ± 0.019	21.870 ± 0.489	21.103 ± 0.140	8.56e-05	1.73e-04		
04120334+2049527	42	M4.5	11.732 ± 0.022	>23.050	21.710 ± 0.094	<6.76e-05	2.32e-04		
04120760+1737341	50	M3.0	10.275 ± 0.023	>22.276	21.165 ± 0.266	<3.61e-05	1.00e-04		
04122173+1615033	52	M2.5	9.736 ± 0.024	>22.038	...	<2.73e-05	...		
04124992+1114462	47	M5.0	12.129 ± 0.021	...	22.302 ± 0.614	...	1.94e-04		
04125498-0518044	40	M3.5	10.943 ± 0.023	>23.611	24.244 ± 0.571	<1.95e-05	1.09e-05		
04130560+1514520	52	M3.5	11.303 ± 0.021	>22.347	...	<8.71e-05	...		
04142981+1843480	47	M2.0	10.294 ± 0.021	>22.348	20.815 ± 0.112	<3.44e-05	1.41e-04		
04144521+1903502	40	M3.5	11.882 ± 0.020	>22.158	22.547 ± 0.302	<1.77e-04	1.23e-04		
04145019+2422375	44	M4.5	12.479 ± 0.020	>22.600	>22.819	<2.04e-04	<1.67e-04		
04153255+2048274	47	M4.5	11.960 ± 0.024	>22.453	>22.835	<1.45e-04	<1.02e-04		
04153447+1935598	40	M4.5	10.787 ± 0.021	21.567 ± 0.293	20.760 ± 0.079	1.11e-04	2.34e-04		
04153482+1645447	52	M3.0	11.050 ± 0.020	>22.004	>22.364	<9.46e-05	<6.79e-05		
04160143+1638592	52	M3.0	10.806 ± 0.022	>22.270	21.792 ± 0.331	<5.92e-05	9.19e-05		
04160357+1851330	53	M2.5	10.247 ± 0.021	>22.228	22.485 ± 0.222	<3.67e-05	2.90e-05		
04161310+1853042	50	K8.0	9.062 ± 0.023	>22.213	20.316 ± 0.056	<1.25e-05	7.18e-05	VB (163 \prime 2)	89
04161352+1647481	47	M4.0	12.058 ± 0.022	>22.067	22.483 ± 0.406	<2.26e-04	1.54e-04	VB (0 \prime 1)	87
04164329+1649203	52	M3.0	11.161 ± 0.022	>21.797	21.883 ± 0.461	<1.27e-04	1.17e-04		

Table 5 *continued*

Table 5 (*continued*)

2MASS Designation	Disc. ^a	Spec.	<i>J</i>	FUV ^b	NUV ^b	<i>f</i> _{FUV} / <i>f</i> _J	<i>f</i> _{NUV} / <i>f</i> _J	Binary?	Binary Ref
Ref	Type	(mag)	(mag)	(mag)	(mag)				
04165445+1621249	50	M2.5	10.434 ± 0.020	>22.510	22.582 ± 0.226	<3.37e-05	3.15e-05		
04173116+3041565	40	M3.5	10.920 ± 0.021	>21.293	>23.325	<1.62e-04	<2.49e-05		
04173969+1224536	52	M3.0	10.746 ± 0.021	>21.915	20.816 ± 0.083	<7.76e-05	2.14e-04	VB (978'8)	90
04174767+1339422	52	K8.5	9.405 ± 0.022	>22.432	21.150 ± 0.097	<1.40e-05	4.57e-05	VB (0'8)	91
04175061+1828307	50	M1.0	9.841 ± 0.022	...	20.691 ± 0.070	...	1.04e-04		
04180852+1319524	52	M2.0	10.288 ± 0.025	>22.472	20.709 ± 0.072	<3.05e-05	1.55e-04	VB (1'6)	90
04181297+1605533	52	M3.5	11.583 ± 0.021	>22.441	21.822 ± 0.124	<1.03e-04	1.83e-04		
04181375+2539395	41	M5.0	12.854 ± 0.020	>22.250	>23.654	<3.97e-04	<1.09e-04		
04183382+1821529	42	M4.0	11.490 ± 0.023	...	22.705 ± 0.276	...	7.44e-05		
04184223+1230385	52	M3.5	11.062 ± 0.020	>21.381	21.518 ± 0.129	<1.70e-04	1.50e-04		
04184345+0315177	40	M5.0	12.183 ± 0.027	>21.924	>22.315	<2.89e-04	<2.02e-04		
04190576+1734235	54	M4.5	12.446 ± 0.022	...	23.532 ± 0.447	...	8.38e-05		
04210061+2431080	42	M3.0	10.786 ± 0.022	>21.995	22.222 ± 0.510	<7.48e-05	6.07e-05		
04211974+1202380	52	M3.5	11.361 ± 0.021	...	22.506 ± 0.247	...	7.94e-05	SB	86
04212344+1052021	42	M3.0	11.049 ± 0.023	>21.698	21.355 ± 0.436	<1.25e-04	1.72e-04		
04215308+2414258	46	M3.0	10.587 ± 0.021	>21.729	22.549 ± 0.442	<7.96e-05	3.74e-05		
04215585+2325058	46	M2.5	9.885 ± 0.024	>22.845	21.395 ± 0.168	<1.49e-05	5.67e-05	VB (91''7)	64
04222503+0337082	40	M2.5	9.857 ± 0.026	21.458 ± 0.502	19.849 ± 0.032	5.22e-05	2.29e-04		
04223004+1026046	48	M0.0	9.511 ± 0.021	>21.360	21.683 ± 0.404	<4.15e-05	3.08e-05		
04225989+1318585	51	M1.0	10.122 ± 0.020	22.075 ± 0.575	20.122 ± 0.194	3.77e-05	2.28e-04		
04232380+1425405	52	M2.5	10.472 ± 0.022	22.481 ± 0.365	20.965 ± 0.076	3.58e-05	1.45e-04		
04232944+1552513	52	M3.0	10.693 ± 0.021	22.899 ± 0.405	22.783 ± 0.293	2.98e-05	3.32e-05		
04235033+1455174	55	M0.0	9.293 ± 0.022	20.634 ± 0.078	18.946 ± 0.021	6.62e-05	3.14e-04		
04235738+2210537	42	M3.5	10.867 ± 0.021	...	21.757 ± 0.546	...	1.00e-04		
04235911+1643178	55	M0.0	9.421 ± 0.022	>23.639	20.990 ± 0.072	<4.68e-06	5.37e-05		
04235950+1122588	49	M3.0	11.091 ± 0.024	>22.138	>22.050	<8.69e-05	<9.42e-05		
04240936+1505155	50	M3.5	10.303 ± 0.021	21.690 ± 0.211	20.996 ± 0.073	6.35e-05	1.20e-04		
04241537+1214500	52	M4.0	11.632 ± 0.021	...	23.261 ± 0.417	...	5.08e-05		
04241843+3825361	40	M4.5	12.141 ± 0.026	>21.999	22.141 ± 0.285	<2.60e-04	2.28e-04		
04242825+1553033	52	M3.0	10.765 ± 0.022	>23.098	...	<2.66e-05	...		
04243838+1554346	52	M3.0	11.335 ± 0.022	>23.111	>23.508	<4.44e-05	<3.08e-05		

Table 5 continued

Table 5 (*continued*)

2MASS Designation	Disc. ^a	Spec.	<i>J</i>	FUV ^b	NUV ^b	<i>f</i> _{FUV} / <i>f</i> _J	<i>f</i> _{NUV} / <i>f</i> _J	Binary?	Binary Ref
Ref	Type	(mag)	(mag)	(mag)	(mag)				
04244401+1046192	53	M2.5	10.304 ± 0.023	...	>21.973	<4.90e-05	
04251652+1618086	52	M4.5	11.867 ± 0.022	>23.295	23.040 ± 0.316	<6.11e-05	7.73e-05		
04251816+2303390	42	M2.5	10.264 ± 0.022	...	21.550 ± 0.375	...	6.97e-05		
04252002+2306312	40	M0.0	9.731 ± 0.021	...	21.518 ± 0.369	...	4.39e-05		
04255043+1500093	52	M4.0	11.629 ± 0.022	>23.451	22.712 ± 0.264	<4.25e-05	8.40e-05		
04260431+1707145	52	M3.5	10.887 ± 0.022	21.067 ± 0.034	20.805 ± 0.022	1.93e-04	2.46e-04		
04261358+4659454	40	M3.5	11.001 ± 0.023	...	>21.762	...	<1.13e-04		
04261903+1703021	47	M5.0	12.870 ± 0.025	>24.585	23.447 ± 0.182	<4.69e-05	1.34e-04		
04270314+2406159	46	M3.5	11.489 ± 0.022	...	>21.424	...	<2.42e-04		
04271663+1714305	52	M1.0	9.714 ± 0.019	>24.800	21.758 ± 0.046	<2.10e-06	3.47e-05		
04273708+2056389	41	M5.0	13.088 ± 0.023	...	>21.871	...	<6.99e-04		
04280370+2424077	40	M4.5	12.249 ± 0.022	...	>21.390	...	<5.02e-04		
04290570+0910569	40	M3.5	12.004 ± 0.021	>21.607	22.453 ± 0.274	<3.28e-04	1.51e-04		
04293738+2140072	56	M2.5	10.227 ± 0.019	...	>22.068	...	<4.18e-05		
04295572+1634506	52	M0.5	9.524 ± 0.023	22.377 ± 0.113	20.506 ± 0.019	1.65e-05	9.22e-05		
04300048+22222304	40	M5.5	12.562 ± 0.021	>21.697	22.351 ± 0.613	<5.05e-04	2.77e-04		
04301702+2622264	42	M3.5	11.803 ± 0.021	...	22.083 ± 0.260	...	1.76e-04		
04302395+1729591	52	M1.5	10.362 ± 0.024	>22.356	21.044 ± 0.263	<3.63e-05	1.22e-04		
04304499+2237482	42	M2.5	10.624 ± 0.026	>21.885	>22.292	<7.13e-05	<4.90e-05		
04305207-0112471	40	M4.5	11.403 ± 0.023	...	22.882 ± 0.366	...	5.83e-05		
04305575+2450174	46	M4.0	11.588 ± 0.022	>22.330	22.531 ± 0.395	<1.15e-04	9.56e-05		
04314362+2109166	40	M4.5	12.654 ± 0.029	>22.271	>22.507	<3.24e-04	<2.61e-04		
04320795+1739522	52	M3.0	10.898 ± 0.021	...	>22.021	...	<8.10e-05		
04322897+1754166	52	M2.5	11.211 ± 0.022	...	21.492 ± 0.417	...	1.76e-04		
04322943+2044078	47	M3.5	11.762 ± 0.027	>22.279	22.765 ± 0.478	<1.41e-04	9.04e-05		
04323784+1902480	46	M3.5	10.794 ± 0.027	...	21.997 ± 0.465	...	7.52e-05		
04330500+2333180	42	M3.5	11.652 ± 0.021	>22.140	22.093 ± 0.588	<1.45e-04	1.52e-04		
04334280+1845592	49	M3.5	10.907 ± 0.020	...	20.114 ± 0.191	...	4.73e-04		
04335544+1822507	47	M4.5	11.849 ± 0.020	...	>21.723	...	<2.56e-04		
04335669+1652087	52	M3.0	10.859 ± 0.020	>24.717	22.896 ± 0.106	<6.52e-06	3.49e-05		
04343908+0638020	42	M3.5	11.725 ± 0.021	>21.650	22.643 ± 0.280	<2.44e-04	9.78e-05		

Table 5 *continued*

Table 5 (*continued*)

2MASS Designation	Disc. ^a	Spec.	<i>J</i> (mag)	FUV ^b (mag)	NUV ^b (mag)	<i>f</i> _{FUV} / <i>f</i> _J	<i>f</i> _{NUV} / <i>f</i> _J	Binary?	Binary Ref
	Ref	Type							
04350555+1310251	52	M3.0	10.675 ± 0.021	>21.828	21.062 ± 0.356	<7.88e-05	1.60e-04		
04352842+1523573	52	M3.5	11.320 ± 0.022	23.581 ± 0.305	22.292 ± 0.153	2.84e-05	9.30e-05		
04353326+1325392	52	M3.0	11.726 ± 0.021	>22.120	>21.650	<1.58e-04	<2.44e-04		
04353850+1317169	52	M2.5	10.731 ± 0.022	>22.122	20.902 ± 0.299	<6.32e-05	1.95e-04		
04355200+1947451	47	M3.0	10.733 ± 0.022	...	21.708 ± 0.431	...	9.28e-05		
04360416+1853189	56	M0.5	9.772 ± 0.022	20.932 ± 0.310	19.704 ± 0.066	7.82e-05	2.42e-04		
04363080+1905273	49	M2.0	10.590 ± 0.022	>21.654	22.030 ± 0.388	<8.55e-05	6.04e-05		
04363893+1836567	56	M1.5	9.777 ± 0.022	>21.708	21.594 ± 0.205	<3.85e-05	4.27e-05		
04370219+4230427	40	M5.0	11.075 ± 0.022	...	>21.933	...	<1.03e-04		
04370517+2043054	40	M3.0	11.113 ± 0.020	...	>21.978	...	<1.03e-04		
04372189+1921175	42	M1.5	10.182 ± 0.023	21.680 ± 0.452	20.322 ± 0.092	5.73e-05	2.00e-04		
04374410+0454066	42	M3.0	10.620 ± 0.024	>21.633	21.251 ± 0.291	<8.96e-05	1.27e-04		
04384339+2144143	46	M4.5	11.950 ± 0.022	>21.939	22.387 ± 0.302	<2.30e-04	1.52e-04		
04385471+1910560	46	M2.0	10.163 ± 0.020	>22.355	20.450 ± 0.094	<3.02e-05	1.75e-04		
04394459-1315008	40	M3.0	11.018 ± 0.023	>21.391	21.353 ± 0.557	<1.62e-04	1.67e-04		
04394496+1805413	47	M5.5	12.689 ± 0.023	>22.582	22.325 ± 0.219	<2.51e-04	3.19e-04		
04395159+1939344	49	M3.5	11.365 ± 0.022	>22.119	22.019 ± 0.152	<1.14e-04	1.25e-04	VB (0'')	87
04395590+2129397	40	M0.5	10.317 ± 0.020	...	22.385 ± 0.255	...	3.39e-05		
04400531+3404031	40	M5.0	12.729 ± 0.021	>22.235	22.336 ± 0.465	<3.59e-04	3.27e-04		
04401271+1917099	50	M1.5	9.948 ± 0.021	>22.067	21.888 ± 0.118	<3.23e-05	3.81e-05		
04402825+1805160	47	M3.5	10.636 ± 0.021	21.898 ± 0.354	21.145 ± 0.079	7.12e-05	1.43e-04		
04403300+1801422	49	M4.0	12.830 ± 0.021	>22.403	>23.462	<3.38e-04	<1.27e-04		
04405203+0905153	40	M4.0	11.696 ± 0.022	>21.663	>22.124	<2.35e-04	<1.54e-04		
04405721+0450544	40	M4.0	12.236 ± 0.021	>21.523	>22.090	<4.39e-04	<2.60e-04		
04410193+1954340	47	M5.5	12.627 ± 0.019	>22.214	22.818 ± 0.245	<3.33e-04	1.91e-04		
04412780+1404340	40	M0.0	9.576 ± 0.021	20.635 ± 0.201	19.685 ± 0.040	8.59e-05	2.06e-04		
04414676+0426122	40	M1.5	10.205 ± 0.027	>21.482	20.739 ± 0.175	<7.03e-05	1.39e-04		
04414687+0716323	42	M3.5	11.537 ± 0.022	...	22.793 ± 0.478	...	7.16e-05		
04421243+1408512	40	M4.0	11.889 ± 0.021	>22.265	21.692 ± 0.313	<1.61e-04	2.73e-04		
04421880+1741383	46	M3.0	10.860 ± 0.024	>22.374	21.806 ± 0.116	<5.65e-05	9.53e-05		
04425093+1929137	46	M3.0	10.822 ± 0.025	...	23.864 ± 0.414	...	1.38e-05		

Table 5 *continued*

Table 5 (*continued*)

2MASS Designation	Disc. ^a	Spec.	<i>J</i> (mag)	FUV ^b (mag)	NUV ^b (mag)	<i>f</i> _{FUV} / <i>f</i> _J	<i>f</i> _{NUV} / <i>f</i> _J	Binary? Ref
	Ref	Type						
04425849+2036174	40	M3.0	10.892 ± 0.025	>22.115	22.741 ± 0.490	<7.39e-05	4.15e-05	
04431267+1518538	40	M0.0	10.248 ± 0.020	>21.669	21.289 ± 0.212	<6.16e-05	8.73e-05	
04431696+0200260	40	M3.0	10.638 ± 0.026	>22.447	22.053 ± 0.154	<4.30e-05	6.19e-05	
04441479+0543573	41	M5.5	13.668 ± 0.023	...	>21.780	...	<1.30e-03	
04442218+3256586	40	M3.5	11.889 ± 0.023	>22.326	>22.322	<1.52e-04	<1.53e-04	
04442835+1751110	49	M3.0	11.579 ± 0.021	>22.195	22.514 ± 0.182	<1.29e-04	9.63e-05	
04443513+1727043	46	M3.5	11.802 ± 0.020	>22.371	>23.546	<1.35e-04	<4.57e-05	
04444376+1824297	49	M2.5	10.561 ± 0.026	>21.088	19.169 ± 0.084	<1.40e-04	8.21e-04	
04450024+1716199	40	M4.0	12.163 ± 0.023	>22.148	>23.374	<2.31e-04	<7.47e-05	
04460271+1928060	41	M5.0	13.237 ± 0.023	>22.023	>22.673	<6.97e-04	<3.83e-04	
04460520+1553241	40	M4.0	11.922 ± 0.021	...	22.674 ± 0.240	...	1.14e-04	
04460918+0645002	40	M2.5	10.395 ± 0.023	...	20.706 ± 0.434	...	1.71e-04	
04460964+1857281	41	M6.0	13.775 ± 0.024	>21.816	>22.189	<1.38e-03	<9.82e-04	
04465287+1253019	40	M3.0	10.896 ± 0.020	>22.232	22.174 ± 0.430	<6.66e-05	7.02e-05	
04465604+3023120	40	M3.5	11.739 ± 0.026	>21.129	>23.674	<3.99e-04	<3.83e-05	
04470974+2401124	48	K9.0	9.281 ± 0.022	...	20.876 ± 0.279	...	5.24e-05	
04471575+1333257	40	M4.5	12.328 ± 0.036	>21.962	>22.273	<3.19e-04	<2.40e-04	
04472420+2239486	40	M5.0	12.883 ± 0.021	>22.435	>22.728	<3.44e-04	<2.63e-04	
04473712+1013587	42	M2.5	10.847 ± 0.022	22.241 ± 0.328	20.769 ± 0.120	6.31e-05	2.45e-04	
04473999–2010338	40	M2.5	10.350 ± 0.022	>23.258	23.124 ± 0.498	<1.56e-05	1.77e-05	
04474965+1241292	42	M3.0	11.337 ± 0.021	>22.244	22.217 ± 0.423	<9.88e-05	1.01e-04	
04475405+0722145	42	M3.5	12.053 ± 0.023	...	>21.901	...	<2.62e-04	
0447546–0047361	41	M6.5	14.063 ± 0.029	>22.535	>23.476	<9.31e-04	<3.91e-04	
04482944+3644031	40	M4.5	12.494 ± 0.021	>22.669	>23.503	<1.94e-04	<8.99e-05	
04482974+2026458	40	M4.5	12.783 ± 0.021	>21.719	>22.234	<6.07e-04	<3.78e-04	
04483062+1623187	42	M0.0	9.415 ± 0.024	>22.272	20.824 ± 0.050	<1.64e-05	6.22e-05	
04483498+1843446	40	M3.5	11.581 ± 0.020	>21.675	>22.243	<2.09e-04	<1.24e-04	
04484599+1123084	41	M5.0	12.504 ± 0.025	>22.551	22.417 ± 0.451	<2.18e-04	2.47e-04	
04485957+1536176	40	M3.0	11.001 ± 0.026	>22.388	22.653 ± 0.233	<6.35e-05	4.97e-05	
04491054+1348414	40	M3.5	11.245 ± 0.024	>21.774	>22.194	<1.40e-04	<9.51e-05	
04492830+1916386	42	M4.0	11.929 ± 0.022	>21.906	>22.237	<2.33e-04	<1.72e-04	

Table 5 continued

Table 5 (*continued*)

2MASS Designation	Disc. ^a	Spec.	<i>J</i> (mag)	FUV ^b (mag)	NUV ^b (mag)	<i>f</i> _{FUV} / <i>f</i> _J	<i>f</i> _{NUV} / <i>f</i> _J	Binary?	Binary Ref
Ref	Type								
04493586+2145391	40	K9.0	10.097 ± 0.021	>22.307	21.153 ± 0.175	<2.98e-05	8.61e-05		
04493656+1701593	40	M4.0	11.652 ± 0.020	>21.869	21.744 ± 0.244	<1.87e-04	2.09e-04		
04495121–1632310	41	M4.0	11.677 ± 0.023	>22.360	22.380 ± 0.647	<1.21e-04	1.19e-04		
04495209+0606336	42	M3.0	10.461 ± 0.021	...	>21.545	...	<8.39e-05		
04495795+2712369	40	M3.5	11.067 ± 0.020	>22.383	21.740 ± 0.323	<6.78e-05	1.23e-04		
04501665+2037330	40	M2.5	10.281 ± 0.021	>21.574	20.325 ± 0.114	<6.92e-05	2.19e-04		
04505946–0008228	40	M4.0	11.858 ± 0.024	>22.415	22.183 ± 0.433	<1.36e-04	1.69e-04		
04515724+0916530	40	M4.5	11.965 ± 0.023	...	>21.609	...	<3.16e-04		
04535700+0915588	42	M4.0	11.308 ± 0.023	...	21.496 ± 0.405	...	1.92e-04		
04543779+0924328	40	M3.5	11.541 ± 0.026	...	>21.608	...	<2.14e-04		
04551484+2121505	40	M4.0	12.169 ± 0.021	>21.958	>22.377	<2.77e-04	<1.88e-04		
04551258+2728384	40	M5.0	12.896 ± 0.022	...	22.163 ± 0.568	...	4.48e-04		
04554665+2114503	40	M3.5	11.777 ± 0.020	>21.977	>22.382	<1.89e-04	<1.30e-04		
04554905+2421458	42	M3.0	10.934 ± 0.021	>22.070	21.708 ± 0.355	<8.00e-05	1.12e-04		
04560611+2153527	40	M5.0	12.877 ± 0.023	>21.624	>23.186	<7.22e-04	<1.71e-04		
04571847+2136085	40	M4.0	12.205 ± 0.021	...	23.601 ± 0.471	...	6.30e-05		
04574644+1628202	40	M3.0	11.438 ± 0.026	18.733 ± 0.094	18.517 ± 0.054	2.75e-03	3.36e-03		
04581370–0246267	40	M4.0	12.056 ± 0.022	...	21.615 ± 0.239	...	3.42e-04		
04582223+1919017	40	M5.0	12.677 ± 0.022	21.310 ± 0.398	>23.433	8.02e-04	<1.14e-04		
04583816+1613206	40	M4.0	11.980 ± 0.024	>21.611	>22.156	<3.20e-04	<1.94e-04		
04590311+1215449	40	M4.5	11.838 ± 0.023	...	21.585 ± 0.134	...	2.88e-04		
04591981+1023096	40	M1.5	10.186 ± 0.024	...	22.104 ± 0.225	...	3.89e-05		
04595855–0333123	40	M1.0	9.759 ± 0.021	20.826 ± 0.340	20.125 ± 0.153	8.52e-05	1.63e-04	VB (0'')	69
05000330+1554531	40	M4.5	11.800 ± 0.023	>21.558	>22.062	<2.85e-04	<1.79e-04		
05001195+0551197	40	M3.0	11.236 ± 0.024	>21.611	19.844 ± 0.123	<1.61e-04	8.21e-04		
05003894+2422581	41	M5.0	13.089 ± 0.021	...	22.112 ± 0.582	...	5.60e-04		
05003970+0907339	41	M4.5	13.091 ± 0.036	>21.542	>21.990	<9.49e-04	<6.28e-04		
05005520+1848267	40	M4.5	12.053 ± 0.022	...	21.748 ± 0.186	...	3.02e-04		
05011599+1608409	40	M4.0	12.567 ± 0.021	>21.597	22.392 ± 0.512	<5.56e-04	2.68e-04		
05013497+0756429	40	M4.5	12.836 ± 0.024	>21.747	>23.118	<6.21e-04	<1.76e-04		
05024838+1337578	40	M4.5	12.766 ± 0.021	>21.603	>21.914	<6.65e-04	<4.99e-04		

Table 5 *continued*

Table 5 (*continued*)

2MASS Designation	Disc. ^a	Spec.	<i>J</i>	FUV ^b	NUV ^b	<i>f</i> _{FUV} / <i>f</i> _J	<i>f</i> _{NUV} / <i>f</i> _J	Binary?	Binary Ref
Ref	Type	(mag)	(mag)	(mag)	(mag)				
05030630+1940436	40	M4.5	12.662 ± 0.023	>21.589	22.100 ± 0.392	<6.12e-04	3.82e-04		
05030708+1901048	40	K8.5	9.225 ± 0.022	>21.880	20.347 ± 0.052	<1.97e-05	8.11e-05		
05031874+1630587	41	M4.5	12.944 ± 0.023	>21.876	22.713 ± 0.297	<6.09e-04	2.82e-04		
05033266+1808525	40	M4.5	12.434 ± 0.021	>21.707	>22.121	<4.45e-04	<3.04e-04		
05034293+1709134	40	M0.0	10.342 ± 0.026	>21.716	21.699 ± 0.219	<6.42e-05	6.53e-05		
05071004+1316112	40	M4.0	11.756 ± 0.027	>21.280	>21.817	<3.53e-04	<2.15e-04		
05073495+1439142	40	M2.5	10.416 ± 0.032	>21.394	20.941 ± 0.252	<9.25e-05	1.40e-04		
05084113+1444397	41	M4.5	13.037 ± 0.027	>21.543	21.323 ± 0.363	<9.02e-04	1.10e-03		
05091578+1934210	40	M1.0	10.797 ± 0.022	>21.723	21.728 ± 0.405	<9.71e-05	9.66e-05		
05094039+0812505	40	M1.5	10.526 ± 0.024	...	20.713 ± 0.231	...	1.92e-04		
05102793+0109080	40	M2.5	11.181 ± 0.024	>21.441	>21.841	<1.79e-04	<1.24e-04		
05105654+1307191	40	M3.0	10.800 ± 0.027	>21.325	21.005 ± 0.097	<1.40e-04	1.89e-04		
05115940+1119417	41	M5.0	13.326 ± 0.024	>21.139	>21.721	<1.71e-03	<9.98e-04		
05122408+1824086	40	K9.0	9.470 ± 0.026	>21.824	20.732 ± 0.240	<2.61e-05	7.12e-05		
05142365+2031537	40	M3.5	11.312 ± 0.029	>23.127	22.159 ± 0.217	<4.28e-05	1.04e-04		
05153017+1725541	40	M4.5	12.629 ± 0.023	>21.584	21.973 ± 0.601	<5.97e-04	4.17e-04		
05161584+0926477	40	M3.0	11.351 ± 0.022	>20.929	>22.948	<3.36e-04	<5.23e-05		
05162552-0031177	40	M4.0	11.595 ± 0.026	...	>21.583	...	<2.30e-04		
05163017-0949505	40	M3.5	11.071 ± 0.024	...	21.612 ± 0.467	...	1.38e-04		
05191461+2407339	41	M4.5	12.842 ± 0.021	...	21.740 ± 0.521	...	6.29e-04		
05220154+1534547	41	M5.0	13.111 ± 0.023	>21.916	22.007 ± 0.347	<6.85e-04	6.30e-04		
05224773+4337494	41	M3.5	11.311 ± 0.023	...	>21.971	...	<1.24e-04		
05231043-0141520	40	M0.0	9.445 ± 0.024	...	>20.964	...	<5.62e-05		
05284754+0152075	40	M3.5	11.231 ± 0.023	...	20.860 ± 0.389	...	3.21e-04		
05380956-0953503	40	M3.5	11.397 ± 0.023	...	21.781 ± 0.578	...	1.60e-04		
05411278+2529131	40	M4.5	12.014 ± 0.021	...	>21.755	...	<2.89e-04	VB (18''/2)	90
05433934+2333025	40	M5.5	12.141 ± 0.024	...	>21.634	...	<3.63e-04		
05540638+2541390	40	M0.5	9.513 ± 0.022	...	21.610 ± 0.458	...	3.30e-05		
06032727+2402152	40	M2.5	10.290 ± 0.021	...	20.428 ± 0.294	...	2.01e-04		
06242410+4331155	41	M2.5	10.343 ± 0.023	>22.643	>22.276	<2.74e-05	<3.84e-05		
06341108+3552005	41	M4.5	12.313 ± 0.024	>22.643	>22.529	<1.68e-04	<1.87e-04		

Table 5 continued

Table 5 (*continued*)

2MASS Designation	Disc. ^a	Spec.	<i>J</i>	FUV ^b	NUV ^b	<i>f</i> _{FUV} / <i>f</i> _J	<i>f</i> _{NUV} / <i>f</i> _J	Binary?	Binary Ref
Ref	Type	(mag)	(mag)	(mag)	(mag)				
Field									
00052423–3721257	...	M1.5	5.328 ± 0.019	23.100 ± 0.559	18.815 ± 0.033	1.77e-07	9.18e-06		
00063325–0732147	...	M5.5	8.323 ± 0.019	22.691 ± 0.440	22.998 ± 0.448	4.08e-06	3.07e-06		
00152799–1608008	...	M3.5	7.215 ± 0.019	>23.289	22.146 ± 0.314	<8.47e-07	2.43e-06		
00182256+4401222	...	M1.5	5.252 ± 0.264	...	18.117 ± 0.053	...	1.63e-05	VB (0'')	92
00244419–2708242	...	M5.5	9.254 ± 0.034	21.258 ± 0.216	...	3.60e-05	...	VB (<0'1, 1'1, 1'5)	94, 95
01102281–6726425	...	M2.5	5.997 ± 0.019	21.695 ± 0.324	19.401 ± 0.068	1.20e-06	9.91e-06	VB (0'')	96
01123052–1639570	...	M4.5	7.258 ± 0.020	20.591 ± 0.188	19.710 ± 0.080	1.06e-05	2.38e-05		
01390120–1757026	...	M5.5	6.283 ± 0.019	17.976 ± 0.005	17.806 ± 0.003	4.79e-05	5.60e-05	VB (2'')	64
02001278+1303112	...	M4.5	7.514 ± 0.017	20.930 ± 0.212	19.663 ± 0.030	9.80e-06	3.15e-05		
02441537+2531249	...	M3.0	6.752 ± 0.018	>22.164	20.334 ± 0.136	<1.56e-06	8.41e-06		
02451431–4344102	...	M4.0	8.059 ± 0.024	20.332 ± 0.159	19.416 ± 0.067	2.81e-05	6.52e-05	VB (0'5, 44'7)	65, 97
02530084+1652532	...	M6.0	8.394 ± 0.027	>22.219	>22.423	<6.72e-06	<5.57e-06		
03015107–1635306	...	M2.5	7.110 ± 0.019	20.499 ± 0.060	19.071 ± 0.020	1.00e-05	3.74e-05	VB (7'')	98
03393521–3525440	...	M9.0	10.725 ± 0.021	>24.854	24.101 ± 0.279	<5.08e-06	1.02e-05		
04102815–5336078	...	M4.5	8.747 ± 0.030	21.381 ± 0.330	...	2.01e-05	...		
04311147+5858375	...	M4.0	6.622 ± 0.021	>22.658	...	<8.77e-07	...	VB (6'8)	99
05114046–4501051	...	M1.0	5.821 ± 0.026	>22.057	19.103 ± 0.049	<7.30e-07	1.11e-05		
05172292–3521545	...	M4.0	7.400 ± 0.026	19.162 ± 0.088	17.843 ± 0.033	4.49e-05	1.51e-04		
05312734–0340356	...	M1.5	4.999 ± 0.300	...	17.003 ± 0.042	...	3.60e-05		
05332802–4257205	...	M4.5	7.997 ± 0.027	20.286 ± 0.248	18.912 ± 0.074	2.77e-05	9.80e-05		
06011106+5935508	...	M3.5	7.465 ± 0.023	>22.568	>22.965	<2.07e-06	<1.44e-06		
06574663–4417281	...	M3.5	6.883 ± 0.019	...	21.070 ± 0.343	...	4.82e-06	VB (0'')	93
06592868+1920577	...	M5.0	9.160 ± 0.024	...	>21.551	...	<2.52e-05		
07100180+3831457	...	M4.5	6.731 ± 0.026	19.975 ± 0.129	18.237 ± 0.013	1.15e-05	5.69e-05		
07272450+0513329	...	M3.5	5.714 ± 0.032	21.703 ± 0.276	20.031 ± 0.034	9.16e-07	4.27e-06		
07401183–4257406	...	M4.5	8.681 ± 0.027	...	20.275 ± 0.244	...	5.25e-05		
08115757+0846220	...	M4.0	8.424 ± 0.023	>22.573	22.282 ± 0.674	<4.99e-06	6.52e-06		
08124088–2133056	...	M3.5	7.601 ± 0.020	...	19.789 ± 0.177	...	3.04e-05		
08294949+2646348	...	M6.5	8.235 ± 0.021	>22.492	17.492 ± 0.031	<4.52e-06	4.52e-04		
08581519+1945470	...	M5.5	7.791 ± 0.023	20.994 ± 0.085	19.678 ± 0.030	1.19e-05	4.00e-05	VB (1'8)	100

Table 5 *continued*

Table 5 (*continued*)

2MASS Designation	Disc. ^a	Spec.	<i>J</i>	FUV ^b	NUV ^b	<i>f</i> _{FUV} / <i>f</i> _J	<i>f</i> _{NUV} / <i>f</i> _J	Binary?	Binary Ref
Ref	Type	(mag)	(mag)	(mag)	(mag)				
08585633+0828259	...	M3.5	6.507 ± 0.018	18.839 ± 0.017	17.485 ± 0.006	2.66e-05	9.25e-05	SB, VB (0'')	87, 70
09002359+2150054	...	M6.0	9.436 ± 0.020	22.646 ± 0.165	21.442 ± 0.077	1.18e-05	3.59e-05		
09142298+5241125	...	M0.0	4.889 ± 0.037	19.539 ± 0.171	16.365 ± 0.016	3.14e-06	5.85e-05	VB (17'')	101
09153642−1035470	...	M5.0	8.605 ± 0.027	21.209 ± 0.076	20.693 ± 0.189	2.07e-05	3.33e-05	VB (0'')	102
09445422−1220544	...	M5.0	8.496 ± 0.024	20.401 ± 0.223	19.145 ± 0.087	3.94e-05	1.25e-04		
10121768−0344441	...	M2.0	5.888 ± 0.021	20.828 ± 0.180	18.178 ± 0.036	2.41e-06	2.76e-05		
10193634+1952122	...	M5.0	5.449 ± 0.027	...	15.814 ± 0.017	...	1.63e-04		
10285555+0050275	...	M2.0	6.176 ± 0.024	21.301 ± 0.064	19.006 ± 0.012	2.03e-06	1.68e-05		
10481258−1120082	...	M6.5	8.857 ± 0.021	>22.799	21.789 ± 0.445	<6.04e-06	1.53e-05		
10481463−3956062	...	M8.5	9.538 ± 0.022	>21.977	21.192 ± 0.336	<2.41e-05	4.96e-05		
10505201+0648292	...	M4.0	7.319 ± 0.023	>25.733	21.121 ± 0.298	<9.82e-08	6.87e-06		
10551532−7356091	...	M7.0	10.630 ± 0.023	>21.576	21.943 ± 0.319	<9.53e-05	6.79e-05		
10562886+0700527	...	M6.0	7.085 ± 0.024	20.654 ± 0.320	18.764 ± 0.010	8.51e-06	4.85e-05		
11000432+2249592	...	M2.5	6.314 ± 0.023	22.071 ± 0.471	19.657 ± 0.077	1.13e-06	1.05e-05		
11032023+3558117	...	M2.0	4.203 ± 0.242	20.217 ± 0.200	17.324 ± 0.028	8.95e-07	1.29e-05		
11052903+4331357	...	M1.0	5.538 ± 0.019	22.471 ± 0.200	18.663 ± 0.018	3.84e-07	1.28e-05	VB (31'')	93
11474143+7841283	...	M3.5	6.724 ± 0.024	>22.650	21.456 ± 0.211	<9.71e-07	2.92e-06		
11474440+0048164	...	M4.0	6.505 ± 0.023	22.964 ± 0.187	21.606 ± 0.065	5.94e-07	2.08e-06		
11505787+4822395	...	M7.0	8.488 ± 0.029	>22.933	22.366 ± 0.194	<3.80e-06	6.40e-06		
12141654+0037263	...	M5.0	8.456 ± 0.026	21.000 ± 0.054	19.663 ± 0.021	2.19e-05	7.49e-05		
12185939+1107338	...	M5.0	8.525 ± 0.027	20.748 ± 0.206	19.488 ± 0.019	2.94e-05	9.39e-05		
12331738+0901157	...	M5.5	6.995 ± 0.024	19.622 ± 0.023	18.329 ± 0.007	2.03e-05	6.67e-05	VB (0'')	103
12384914−3822527	...	M4.0	8.174 ± 0.024	>21.871	21.950 ± 0.164	<7.56e-06	7.03e-06		
12404633−4333595	...	M3.0	8.217 ± 0.029	>22.010	>22.288	<6.92e-06	<5.36e-06		
12590470−4336243	...	M8.0	10.534 ± 0.022	>21.758	22.274 ± 0.533	<7.38e-05	4.59e-05		
13295979+1022376	...	M1.0	5.902 ± 0.018	>22.015	18.439 ± 0.015	<8.17e-07	2.20e-05		
1345354+1453317	...	M1.5	5.181 ± 0.037	20.603 ± 0.244	18.113 ± 0.012	1.54e-06	1.53e-05		
14294291−6240465	...	M5.5	5.357 ± 0.023	...	18.601 ± 0.086	...	1.15e-05	VB (7840'')	104
16252459+5418148	...	M1.5	6.608 ± 0.020	>22.839	20.064 ± 0.071	<7.33e-07	9.44e-06		
16311879+4051516	...	M5.0	9.461 ± 0.023	21.484 ± 0.035	20.444 ± 0.010	3.53e-05	9.21e-05		
17093153+4340531	...	M3.5	7.380 ± 0.019	21.848 ± 0.407	...	3.72e-06	...		

Table 5 *continued*

Table 5 (*continued*)

2MASS Designation	Disc. ^a	Spec.	<i>J</i> (mag)	FUV ^b (mag)	NUV ^b (mag)	<i>f</i> _{FUV} / <i>f</i> _J	<i>f</i> _{NUV} / <i>f</i> _J	Binary?	Binary Ref
	Ref	Type							
17185868–3459483	...	M1.5	6.848 ± 0.021	...	>21.896	...	<2.18e-06	VB (30'')	105
17370367–4419088	...	M3.5	6.544 ± 0.023	...	19.298 ± 0.072	...	1.80e-05	VB (0'')	90
17463427–5719081	...	M2.0	6.855 ± 0.021	>21.810	...	<2.37e-06	...		
18021660+6415445	...	M5.0	8.541 ± 0.024	20.693 ± 0.193	19.675 ± 0.087	3.14e-05	8.02e-05		
18050755–0301523	...	M0.0	6.161 ± 0.019	...	19.029 ± 0.082	...	1.62e-05		
18111528–7859227	...	M4.5	7.840 ± 0.019	...	18.673 ± 0.014	...	1.06e-04		
18185725+6611332	...	M4.5	8.740 ± 0.021	21.895 ± 0.453	20.859 ± 0.125	1.25e-05	3.24e-05		
18353790+3259545	...	M8.5	10.270 ± 0.022	>23.828	21.505 ± 0.036	<8.60e-06	7.30e-05		
18424666+5937499	...	M3.0	5.189 ± 0.017	21.032 ± 0.274	19.133 ± 0.023	1.05e-06	6.03e-06	VB (12'')	93
18424688+5937374	...	M3.5	5.721 ± 0.020	...	19.221 ± 0.025	...	9.07e-06	VB (12'')	93
18450079–1409036	...	M5.0	8.461 ± 0.034	...	19.640 ± 0.091	...	7.69e-05	VB (3'')	18
18494929–2350101	...	M3.5	6.222 ± 0.018	19.264 ± 0.093	17.858 ± 0.031	1.38e-05	5.05e-05		
18522528–3730363	...	M4.5	8.377 ± 0.035	21.070 ± 0.340	19.398 ± 0.111	1.91e-05	8.89e-05		
20133335–4509506	...	M0.0	5.122 ± 0.023	20.277 ± 0.120	16.922 ± 0.014	1.97e-06	4.34e-05		
20294834+0941202	...	M4.5	8.228 ± 0.020	20.634 ± 0.208	19.711 ± 0.094	2.48e-05	5.81e-05	VB (<0'')	106
20303207+6526586	...	M2.5	6.735 ± 0.021	>21.707	19.273 ± 0.079	<2.34e-06	2.20e-05		
20360829–3607115	...	M4.5	8.026 ± 0.023	19.759 ± 0.121	18.382 ± 0.043	4.62e-05	1.64e-04		
21293671+1738353	...	M3.5	6.249 ± 0.021	>21.565	20.060 ± 0.038	<1.70e-06	6.81e-06		
21333397–4900323	...	M1.5	5.349 ± 0.032	20.687 ± 0.168	18.393 ± 0.036	1.67e-06	1.38e-05		
22011310+2818248	...	M3.5	7.635 ± 0.026	18.507 ± 0.077	17.400 ± 0.028	1.02e-04	2.83e-04		
22230696–1736250	...	M4.5	8.242 ± 0.027	20.496 ± 0.225	19.344 ± 0.056	2.86e-05	8.25e-05		
22383372–1517573	...	M5.0	6.553 ± 0.019	20.606 ± 0.136	19.701 ± 0.057	5.45e-06	1.25e-05	SB, VB (0'')	87, 107
22480446–2422075	...	M4.0	8.075 ± 0.023	20.922 ± 0.196	19.206 ± 0.043	1.66e-05	8.04e-05		
22531672–1415489	...	M3.5	5.934 ± 0.019	22.560 ± 0.360	20.149 ± 0.087	5.10e-07	4.69e-06		
22563497+1633130	...	M1.5	5.360 ± 0.020	20.829 ± 0.211	...	1.48e-06	...		
23055131–3551130	...	M0.5	4.338 ± 0.258	20.326 ± 0.203	16.874 ± 0.027	9.17e-07	2.20e-05		
23315208+1956142	...	M3.5	6.162 ± 0.024	17.725 ± 0.044	...	5.40e-05	...		
23351050–0223214	...	M5.5	9.148 ± 0.021	21.484 ± 0.135	20.327 ± 0.061	2.65e-05	7.69e-05		
23415498+4410407	...	M5.5	6.884 ± 0.026	...	21.288 ± 0.399	...	3.94e-06		
23491255+0224037	...	M1.0	5.827 ± 0.023	21.690 ± 0.124	18.810 ± 0.017	1.03e-06	1.46e-05		

Table 5 continued

Table 5 (*continued*)

2MASS Designation	Disc. ^a	Spec.	<i>J</i>	FUV ^b	NUV ^b	<i>f</i> _{FUV} / <i>f</i> _J	<i>f</i> _{NUV} / <i>f</i> _J	Binary?	Binary Ref
Ref	Type	(mag)	(mag)	(mag)	(mag)				
References —(1) Riedel (2012), (2) Schneider et al. (2012b), (3) Kastner et al. (1997), (4) Sterzik et al. (1999), (5) Looper et al. (2010a), (6) Looper et al. (2010b), (7) Webb et al. (1999), (8) Donaldson et al. (2016), (9) Gagné et al. (2015a), (10) Gagné et al. (2015b), (11) Song et al. (2003), (12) Shkolnik et al. (2011), (13) Reid (2003), (14) Zuckerman et al. (2001), (15) Shkolnik et al. (2017), (16) Malo et al. (2013), (17) Lépine & Simon (2009), (18) Malo et al. (2014), (19) Kiss et al. (2011), (20) Binks & Jeffries (2016), (21) Elliott et al. (2016), (22) Schlieder et al. (2014), (24) Rodriguez et al. (2014), (25) Riedel et al. (2014), (26) Schlieder et al. (2012a), (27) Barrado y Navascués et al. (1999), (28) Alonso-Floriano et al. (2015), (29) Torres et al. (2008), (30) Kraus et al. (2014), (31) Delorme et al. (2013), (32) Rodriguez et al. (2013), (33) Torres et al. (2000), (34) Shkolnik et al. (2012), (35) McCarthy & White (2012), (36) Riedel et al. (2017), (37) Zuckerman et al. (2004), (38) Schlieder et al. (2012b), (39) Nakajima et al. (2010), (40) Röser et al. (2011), (41) Goldman et al. (2013), (42) Weis & Hanson (1988), (43) Crain et al. (1986), (44) Eggen (1993), (45) Giclas et al. (1962), (46) Upgren et al. (1985), (47) Reid (1992), (48) Weis et al. (1979), (49) Reid (1993), (50) Johnson et al. (1962), (51) Hanson (1975), (52) van Altena & Mikkola (2015), (58) Stock & Wroblewski (1972), (59) Konopacky et al. (2007), (60) Weinberger et al. (2013), (61) Gagné et al. (2017), (62) Jayawardhana et al. (2006), (63) Nicholson (2015), (64) Luyten (1997), (65) Bergfors et al. (2010), (66) Szczegiel et al. (2008), (67) Helminiak et al. (2012), (68) Ianna (1979), (69) Janson et al. (2012), (70) Delfosse et al. (1999), (71) Pasquini et al. (1989), (72) Hartkopf et al. (2013), (73) Bowler et al. (2015), (74) Janson et al. (2017), (75) Shan et al. (2017), (76) Chauvin et al. (2010), (77) McCarthy et al. (2001), (78) Bowler et al. (2013), (79) Jao et al. (2003), (80) Reid & Walkowicz (2006), (81) Law et al. (2006), (82) Gálvez et al. (2006), (83) Lowrance et al. (2005), (84) Bowler et al. (2012), (85) Law et al. (2008), (86) Reid & Maloney (2000), (87) Reid & Gizis (1997), (88) Bender & Simon (2008), (89) Miret & Tobal (2009), (90) Mason et al. (2001), (91) Guenther et al. (2005), (92) Heintz (1987), (93) Eggen (1956), (94) Leinert et al. (1994), (95) Henry et al. (1999), (96) Golinowski et al. (2004), (97) Jeffers et al. (1963), (98) Gliese & Jahreiß (1991), (99) Giclas et al. (1965), (100) Gliese & Jahreiß (1979), (101) Guntzel-Lügner (1955), (102) Monnagnier et al. (2006), (103) Reuyl (1941), (104) Innes (1915), (105) Herschel (1847), (106) Harrington (1971), (107) Leinert et al. (1986), (108) Hopmann (1948)									

^a Discovery references refer to the first publication to suggest cluster or moving group membership. Because the field sample is a volume-limited sample and not a coeval cluster or group, we do not include discovery references for this sample.

^b If an object has no value given for either FUV or NUV, it was either not covered by that detector or had only detections with bad photometric contamination flags.

APPENDIX

A. CONVERTING *GALEX* FLUX DENSITIES TO FLUXES

If one wishes to convert flux density to flux (in erg cm⁻² s⁻¹), one can use the following formula:

$$f_{\text{NUV,FUV}} = (f_{\text{NUV,FUV}})c\lambda_{\text{eff}}^{-2}\Delta\lambda \quad (\text{A1})$$

where $f_{\text{NUV,FUV}}$ is the flux density (in μJy), c is the speed of light, λ_{eff} is the effective filter wavelength, and $\Delta\lambda$ is the filter width. *GALEX* documentation gives $\lambda_{\text{eff}} = 2267 \text{ \AA}$ and $\Delta\lambda = 732 \text{ \AA}$ for *GALEX* NUV, and $\lambda_{\text{eff}} = 1516 \text{ \AA}$ and $\Delta\lambda = 268 \text{ \AA}$ for *GALEX* FUV⁶. Note that the flux emitted from low-mass stars in these bands is primarily from spectral lines that originate in the chromosphere and transition region of their atmospheres. For the NUV band in particular, much of the flux comes from Fe II lines that occur in the red side of the detector bandpass. The amount of flux from these lines, which varies for each star, could shift the λ_{eff} , affecting the resulting flux measurements.

In order to determine the effects of M dwarf spectral shapes on λ_{eff} values, we gathered UV spectra of M dwarfs from the MUSCLES *HST* program (France et al. 2013, France et al. 2016). Using equation A2 of Tokunaga & Vacca (2005) and the *GALEX* filter response curves⁷, we calculate λ_{eff} values for seven M dwarfs with spectral types ranging from M1.5 to M5.5. We exclude the M4.5 dwarf GJ 1214 because of the low S/N of its spectrum. The results are shown in Table A1 and Figure A1. Though the sample size is small, λ_{eff} values tend to decrease with later spectral type. While the FUV λ_{eff} values bracket the *GALEX* provided λ_{eff} value, the calculated λ_{eff} values for the NUV band are clearly distinct from the *GALEX* provided value. We find average λ_{eff} values for the FUV and NUV bands of 1542.8 \AA and 2553.4 \AA , respectively.

Table 6. λ_{eff} for MUSCLES M Dwarfs and *GALEX* Filters

Star Name	Spectral Type	FUV (\AA)	NUV (\AA)
GJ 667C	M1.5	1605.2	2543.9
GJ 832	M1.5	1569.4	2612.9
GJ 176	M2.5	1553.6	2583.3
GJ 436	M3.5	1494.9	2551.2
GJ 581	M5	1503.6	2602.1
GJ 876	M5	1518.9	2528.2
GJ 551	M5.5	1553.9	2452.2

⁶ <http://galex.stsci.edu/gr6/?page=faq>

⁷ <https://asd.gsfc.nasa.gov/archive/galex/Documents/PostLaunchResponseCurveData.html>

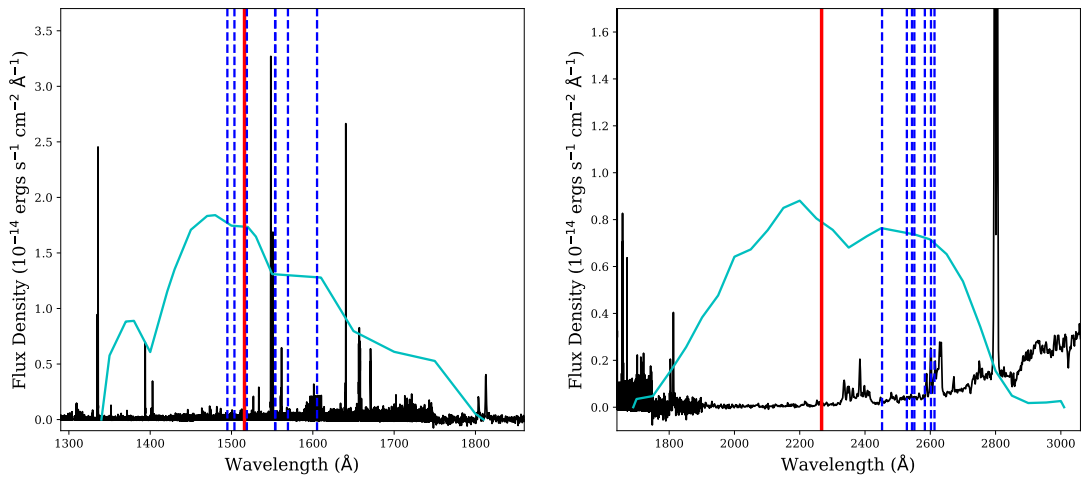


Figure 14. Filter profiles of the *GALEX* FUV (left) and NUV (right) bandpasses (arbitrarily scaled). The spectrum of the M2.5 dwarf GJ 176 from the MUSCLES program (France et al. 2013, France et al. 2016) is overplotted for comparison purposes. The effective wavelength provided in the *GALEX* documentation is show as a solid red line, while the effective wavelengths determined for M dwarfs in the MUSCLES sample are show as blue dashed lines.